

Article

Discovery of Clinical Candidate (5-(3-(4-Chlorophenoxy)prop-1-yn-1-yl)-3-hydroxypicolinoyl)glycine, an Orally Bioavailable Prolyl Hydroxylase Inhibitor for the Treatment of Anemia

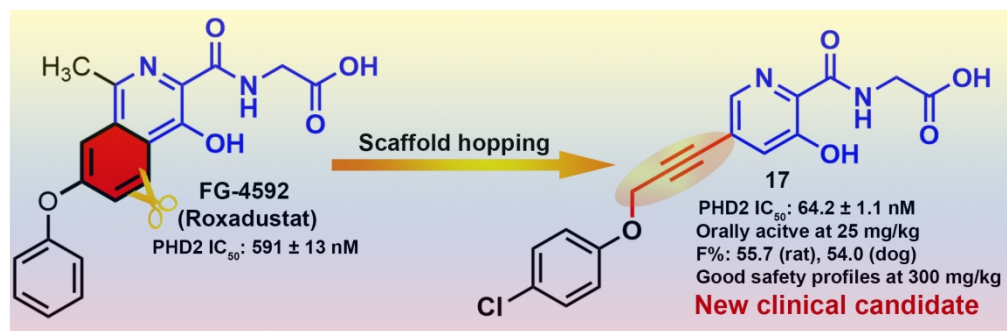
Xiaojin Zhang, Yonghua Lei, Tianhan Hu, Yue Wu, Zhihong Li,
Zhensheng Jiang, Changyong Yang, Lianshan Zhang, and Qi-Dong You

J. Med. Chem., **Just Accepted Manuscript** • DOI: 10.1021/acs.jmedchem.0c01161 • Publication Date (Web): 28 Jul 2020

Downloaded from pubs.acs.org on July 28, 2020

Just Accepted

“Just Accepted” manuscripts have been peer-reviewed and accepted for publication. They are posted online prior to technical editing, formatting for publication and author proofing. The American Chemical Society provides “Just Accepted” as a service to the research community to expedite the dissemination of scientific material as soon as possible after acceptance. “Just Accepted” manuscripts appear in full in PDF format accompanied by an HTML abstract. “Just Accepted” manuscripts have been fully peer reviewed, but should not be considered the official version of record. They are citable by the Digital Object Identifier (DOI®). “Just Accepted” is an optional service offered to authors. Therefore, the “Just Accepted” Web site may not include all articles that will be published in the journal. After a manuscript is technically edited and formatted, it will be removed from the “Just Accepted” Web site and published as an ASAP article. Note that technical editing may introduce minor changes to the manuscript text and/or graphics which could affect content, and all legal disclaimers and ethical guidelines that apply to the journal pertain. ACS cannot be held responsible for errors or consequences arising from the use of information contained in these “Just Accepted” manuscripts.



1
2
3
4
5
6
7 Discovery of Clinical Candidate (5-(3-(4-
8
9
10 Chlorophenoxy)prop-1-yn-1-yl)-3-
11
12
13
14
15 hydroxypicolinoyl)glycine, an Orally Bioavailable
16
17
18
19 Prolyl Hydroxylase Inhibitor for the Treatment of
20
21
22
23
24 Anemia
25
26
27

28
29 *Xiaojin Zhang,^{a,c,1,*} Yonghua Lei,^{a,b,1} Tianhan Hu,^{a,b} Yue Wu,^{a,b} Zhihong Li,^c Zhensheng Jiang,^{a,b}*
30
31 *Changyong Yang,^d Lianshan Zhang,^d Qidong You^{a,b,*}*
32
33
34
35
36

37
38 ^a State Key Laboratory of Natural Medicines and Jiangsu Key Laboratory of Drug Design and
39
40 Optimization, China Pharmaceutical University, Nanjing 210009, China
41
42

43 ^b Department of Medicinal Chemistry, China Pharmaceutical University, Nanjing 211198, China
44
45

46 ^c Department of Chemistry, China Pharmaceutical University, Nanjing 211198, China
47
48

49 ^d Shanghai Hengrui Pharmaceutical Co., Ltd., Shanghai 200245, China
50
51
52
53
54
55
56
57
58
59
60

ABSTRACT

The design and discovery of a new series of (5-alkynyl-3-hydroxypicolinoyl)glycine inhibitors of prolyl hydroxylase (PHD) is described. These compounds showed potent *in vitro* inhibitory activity toward PHD2 in a fluorescence polarization-based assay. Remarkably, oral administration of **17**, with an IC₅₀ of 64.2 nM toward PHD2, was found to stabilize HIF- α , elevate erythropoietin (EPO), and alleviate anemia in a cisplatin-induced anemia mouse model with an oral dose of 25 mg/kg. Rat and dog studies showed that **17** has good pharmacokinetic properties, with an oral bioavailability of 55.7% and 54.0%, respectively, and shows excellent safety profiles even at a high dose of 200 mg/kg in these animals. Based on these results, **17** is currently being evaluated in a phase I clinical trial for anemia.

KEYWORDS

HIF, PHD inhibitor, anemia, EPO

1. INTRODUCTION

Anemia is a condition characterized by abnormally reduced levels of circulating red blood cells (RBCs), or by the presence of RBCs that do not contain enough hemoglobin (Hb); as a result, an insufficient amount of oxygen reaches tissues and organs.¹ Anemia is highly prevalent in patients with chronic kidney disease (CKD) and cancer patients receiving chemotherapy. Over recent decades, intravenous (*iv*) or subcutaneous injection of recombinant human erythropoietin (rhEPO) or its analogs has been considered as the standard of care for renal anemia.² However, exogenous rhEPO injection may cause serious cardiovascular side effects and intravenous iron as an adjuvant

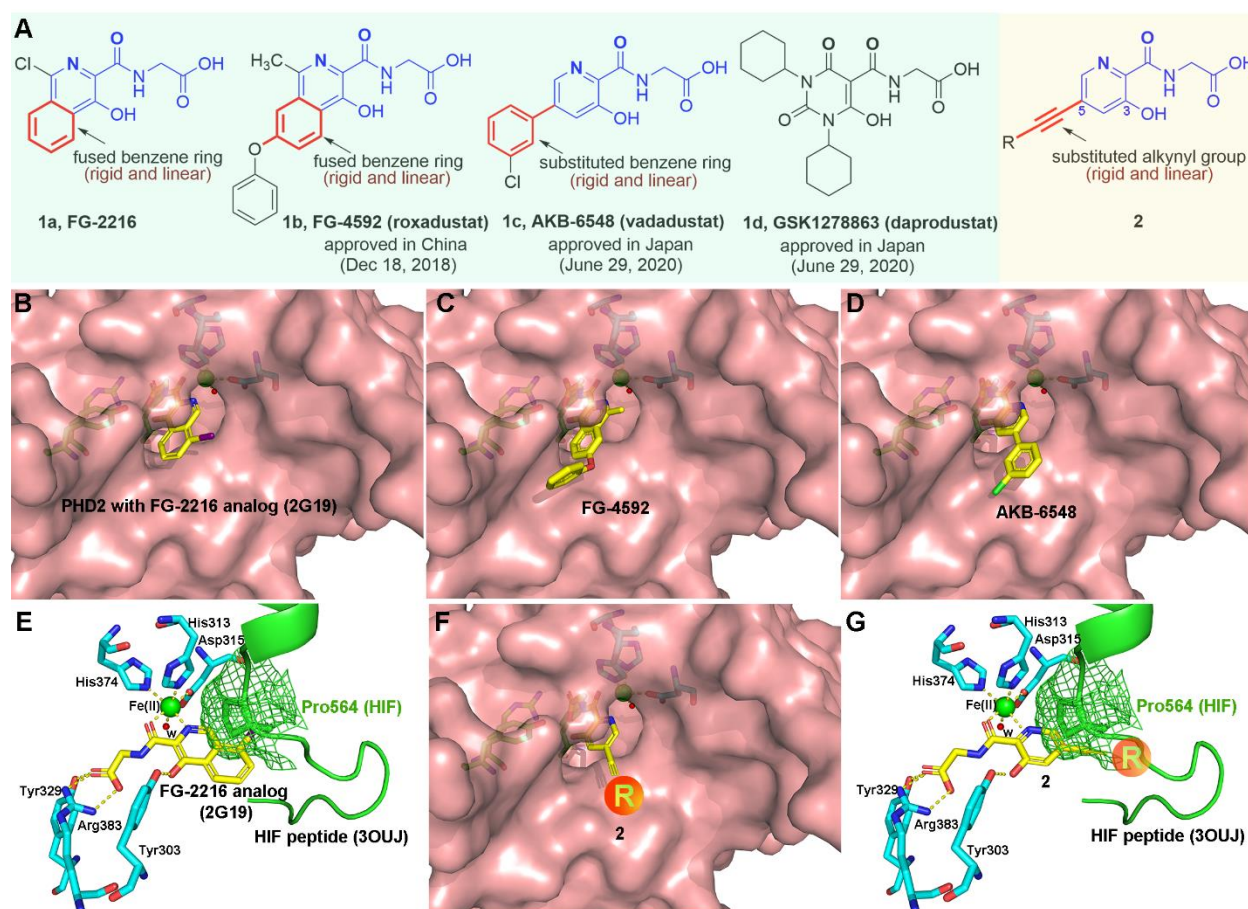
1
2
3 therapy is generally required.³ Recently, orally-active small molecule inhibitors of prolyl
4 hydroxylases (PHDs) have been clinically validated as novel and effective therapies for anemia.
5
6 Their mechanism of action is through the upregulation of endogenous EPO, thus overcoming the
7
8 side effects of rhEPO therapy.^{4, 5}
9
10

11
12
13 PHDs (PHD1-3 enzymes) are a family of iron-, 2-oxoglutarate (2-OG)-, and oxygen-
14 dependent dioxygenases. PHDs act as direct cell oxygen sensors to control the degradation of
15 hypoxia-inducible factor (HIF),⁶ a crucial heterodimeric gene transcription factor involved in
16 endogenous EPO formation and erythropoiesis.⁷ Under normoxic conditions, HIF- α , the regulatory
17 subunit of the HIF dimer, can be post-transcriptionally hydroxylated on certain proline residues,
18 catalyzed by PHD enzymes; the hydroxyl form of HIF- α is precisely recognized by the von
19 Hippel–Lindau tumor suppressor protein (pVHL), causing ubiquitin-mediated proteasomal
20 degradation.⁸ Among the three PHD subtypes (PHD1, PHD2, and PHD3), PHD2 is the most
21 widely distributed isoform, playing a dominant role in regulating steady-state HIF- α and its
22 downstream gene expression, such as EPO.^{9, 10} Inhibiting PHD2 is considered to be an effective
23 strategy to upregulate the endogenous EPO level for the treatment of anemia.
24
25
26
27
28
29
30
31
32
33
34
35
36
37
38
39

40 Over the past two decades, an increasing number of PHD2 inhibitors have been
41 developed.^{5,10,11} To date, over ten PHD2 inhibitors have been subjected to clinical trials¹⁰ and three
42 of them have been approved.¹²⁻¹⁶ **FG-2216 (1a)** (Figure 1A) was the first PHD2 inhibitor to enter
43 clinical trials from FibroGen.¹⁰ **FG-4592 (1b, roxadustat)** (Figure 1A), structurally related to **FG-**
44 **2216** and also originally from FibroGen, was approved by the National Medical Products
45 Administration (NMPA) in China in December 2018 as a first-in-class PHD inhibitor for the
46 treatment of CKD-related anemia.¹²⁻¹⁴ Recently, on June 29, 2020, **AKB-6545 (1c, vadadustat)**¹⁵
47 and **GSK1278863 (1d, daprodustat)**¹⁶ (Figure 1A), originally from Akebia and GlaxoSmithKline,
48
49
50
51
52
53
54
55
56
57
58
59
60

respectively, were approved in Japan for the treatment of anemia due to CKD in dialysis-dependent and non-dialysis-dependent adult patients.

Structurally, all of the PHD2 inhibitors in clinical trials or approved act as mimetics of the endogenous cofactor 2-OG. The co-crystal structure (PDB ID: 2G19)¹⁷ of a reported **FG-2216**-like inhibitor with PHD2 revealed that the 3-hydroxylpicolinoylglycine moiety (marked in blue, Figure 1A) in **1a-1c** share three key interactions with the PHD2 catalytic pocket, including bidentate coordination with ferrous ion, an ionic bonding interaction between carboxylic and Arg383, and a hydrogen bonding interaction between phenol and Tyr303 (Figure 1B and 1E).^{17, 18}



1
2
3 **Figure 1.** (A) Chemical structures of **FG-2216 (1a)**, the approved drugs **FG-4592 (1b)**, **AKB-**
4 **6548 (1c)**, and **GSK1278863 (1d)**, and the alkynyl-containing compound (**2**) designed in this work.
5
6 (B) Binding pose of a reported **FG-2216**-like inhibitor (yellow) with PHD2 (brown) from the X-
7 ray co-crystal structure (PDB ID: 2G19)¹⁷. (C) Predicted binding pose of **FG-4592** (yellow) with
8 PHD2. (D) Predicted binding pose of **AKB-6548** (yellow) with PHD2. (E) Binding mode of the
9 **FG-2216**-like inhibitor (yellow) with the key residues (blue) in PHD2 catalytic sites (PDB ID:
10 2G19)¹⁷ and a superimposition with HIF peptide (green) that has been extracted from a PHD2-
11 HIF- α peptide complex (PDB ID: 3OUJ)¹⁸. The binding mode indicates that the 3-
12 hydroxypicolinoylglycine moiety is the key pharmacophoric group binding to the PHD2 catalytic
13 site while the fused benzene ring and the phenyloxy substituent in **FG-4592** and the substituted
14 benzene ring in **AKB-6548** are probably responsible for preventing HIF from approaching the
15 PHD2 catalytic sites. (F) Predicted binding pose of **2** (yellow) with PHD2. (G) Predicted binding
16 mode of **2** (yellow) with the key residues (blue) in PHD2 catalytic sites (PDB ID: 2G19) and a
17 superimposition with HIF peptide (green) that has been extracted from a PHD2-HIF- α peptide
18 complex (PDB ID: 3OUJ).
19
20
21
22
23
24
25
26
27
28
29
30
31
32
33
34
35
36
37
38

39 Currently, structurally diverse PHD2 inhibitors have been developed by replacing the
40 isoquinone/pyridine cores in **FG-4592/AKB-6548** with other heterocycles, such as quinolinone,¹⁹
41 naphthyridinone,¹⁹ imidazopyridine,²⁰ aza-benzimidazole,²¹ and benzoimidazole,¹⁸ or by changing
42 the formylglycine side chain into thiazole- or pyrazole-substituted carboxylic acids.²²⁻²⁴ Non-
43 carboxylic acid-type inhibitors for PHD2 have also been discovered by high-throughput
44 screening.²⁵⁻²⁷ With regard to the fact that most of these diverse PHD2 inhibitors are still under
45 preclinical study, the 3-hydroxypicolinoylglycine moiety in **FG-4592/AKB-6548** appears to be a
46 privilege scaffold for PHD2 inhibition. Here, we present a new series of alkynyl-containing PHD2
47
48
49
50
51
52
53
54
55
56
57
58
59
60

1
2
3 inhibitors (**2**) designed through the scaffold hopping approach by replacing the rigid and linear
4 isoquinoline core/phenyl pyridine core in **FG-4592**/**AKB-6548** with a rigid and linear 3-akynyl
5 pyridine core (Figure 1A). A fluorescence polarization (FP)-based assay, developed previously
6 using FITC-labeled HIF- α peptide as the probe, was utilized for structure-activity relationship
7 (SAR) optimization in our research.²⁸ Based on the PHD2 inhibitory activity identified *in vitro*,
8 compounds of interest were selected for pharmacodynamic (PD) evaluation to assess their effects
9 on serum EPO *in vivo*. Oral administration of candidate compound **17** was found to stabilize HIF-
10 α , upregulate the endogenous formation of EPO, and effectively mitigate anemia in a cisplatin-
11 induced anemia mouse model. Further, preclinical evidence indicated that **17** has good
12 pharmacokinetic (PK) properties in rats and dogs and excellent early safety profiles in these
13 animals. Thus, **17** appears to be an orally-active clinical candidate for the treatment of anemia.
14
15
16
17
18
19
20
21
22
23
24
25
26
27
28

29 **2. RESULTS AND DISCUSSION**

30 **2.1. Design and SAR optimization by *in vitro* PHD2 inhibitory activity.**

31
32
33 When we conducted this research, the structures of **FG-2216** and **FG-4592** were reported and the
34 scaffold of **AKB-6548** was disclosed. Based on the X-ray structure of a reported **FG-2216**-like
35 inhibitor (yellow) with PHD2 (brown) (PDB ID: 2G19) (Figure 1B),¹⁷ we performed molecular
36 docking studies using GOLD 5.1 software to predict the binding mode of **FG-4592** (Figure 1C)
37 and **AKB-6548** (Figure 1D); as seen, their picolinoylglycine moiety fit deeply into the catalytic
38 pocket of PHD2 (Figure 1B-1D). Further superimposition analysis (Figure 1E) demonstrated the
39 fused benzene ring and phenyloxy substituent in **FG-4592** and the substituted benzene ring in
40 **AKB-6548** oriented to the HIF binding region, suggesting that these rigid fused or substituted
41
42
43
44
45
46
47
48
49
50
51
52
53
54
55
56
57
58
59
60

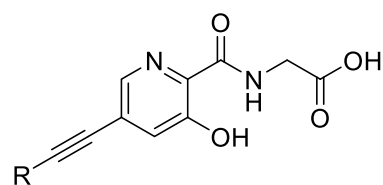
1
2
3 rings on the 3-hydroxypicolinoylglycine scaffold are probably responsible for their inhibitory
4 activity preventing HIF from approaching PHD2 catalytic sites.
5
6

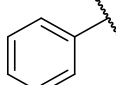
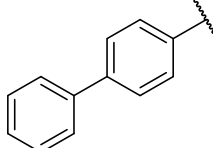
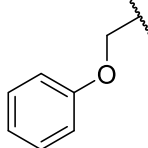
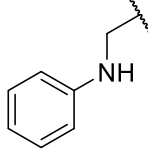
7
8 In light of these findings, we initially designed compound **2** (Figure 1A), which maintains
9 the key pharmacophoric 3-hydroxypicolinoylglycine moiety for PHD2 binding and bears a rigid
10 alkynyl substitution at the C5 site on the picolinoylglycine moiety to allow the extension of suitable
11 substituents and prevent HIF from approaching PHD2 catalytic sites (Figures 1F and 1G). It is
12 worth noting that the methyl group in **FG-4592** was removed because it did not form any important
13 interaction with PHD2 (Figure 1C) and the rigid alkynyl substitution was set at the C5 site because
14 steric clashes with surrounding key residues will arise with C4 or C6 substitutions (Figure S1B-
15 D).
16
17
18
19
20
21
22
23
24
25
26
27

28 Our efforts started with compound **3** with the simplest R group of H. *In vitro* FP-based
29 assays revealed that **3** was a moderately potent inhibitor toward PHD2 with an IC₅₀ value of 2.9
30 μM (Table 1). Nevertheless, this starting compound represented a new scaffold for PHD2
31 inhibition deserving further optimization. Considering that the ethynyl group in **3** oriented to the
32 solvent region of PHD2 and played the role of preventing the HIF substrate from approaching the
33 PHD2 catalytic site, steric substituents such as *tert*-butyl, cyclopropyl, and phenyl groups were
34 introduced to the end of the ethynyl moiety, as seen in **4-6**, respectively. Interestingly, their
35 inhibitory activities toward PHD2 were significantly improved when compared with **3**; the phenyl
36 substituted **6** showed an IC₅₀ value of 820 nM. We then introduced an additional phenyl group to
37 **6**, leading to great loss in activity, as seen in **7** (IC₅₀ = 8103 nM). Because the phenoxy moiety
38 in **1** is relatively flexible, we further introduced an sp³-hybrid methylene group together with an
39 oxygen atom as a rotatable linkage. Encouragingly, the resulting compound, **8**, possessed an IC₅₀
40 value of 169 nM on PHD2 inhibition, turning out to be significantly more active than **6** and even
41
42
43
44
45
46
47
48
49
50
51
52
53
54
55
56
57
58
59
60

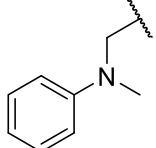
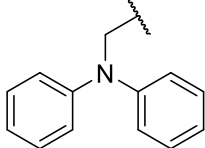
more potent *in vitro* than the approved drug **1** ($IC_{50} = 591$ nM). Replacing the O atom in the linkage of **8** to the NH group was detrimental for activity; compound **9** showed an IC_{50} value toward PHD2 of 326 nM, about two-fold less active than **8**. Introducing methyl or phenyl to the NH moiety, as in **10** and **11**, resulted in further decreases in activity, with IC_{50} values of 454 nM and 651 nM, respectively. Thus, these preliminary SAR data demonstrated that the phenoxy methyl moiety installed at the end of the ethynyl picolinoylglycine scaffold is preferable for PHD2 inhibitory potency as compared to rigid and bulky substituents.

Table 1. Preliminary SAR on the R group



compound	R	PHD2 IC_{50} (nM)
3	H	2900 ± 32
4		1200 ± 56
5		835 ± 3
6		820 ± 11
7		8103 ± 46
8		169 ± 1
9		326 ± 1

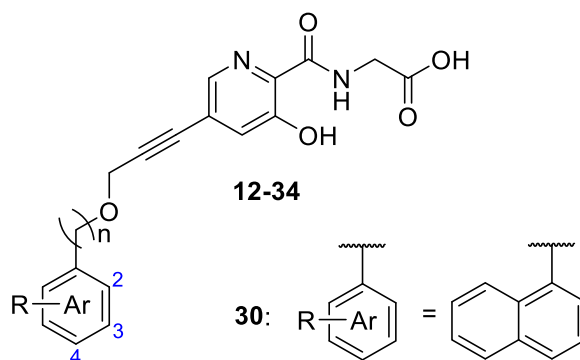
1
2
3
4
5
6
7
8
9
10
11
12
13
14
15
16
17
18
19
20
21
22
23
24
25
26
27
28
29
30
31
32
33
34
35
36
37
38
39
40
41
42
43
44
45
46
47
48
49
50
51
52
53
54
55
56
57
58
59
60

10		454 ± 23
11		651 ± 33
FG-4592 (1)		591 ± 13

Subsequent SAR optimization set out to focus on the phenyl group of **8** (Table 2). Substituents with different electronic properties, including fluoro, chloro, methyl, trifluoromethyl, and methoxy, as in **12-26**, were introduced to *ortho*, *meta*, and *para* sites of the phenyl. It was found that, in all the cases except for methyl, *para* substitution was preferable compared to *ortho* and *meta* substitution for PHD2 inhibitory activity. In particular, **17**, with a *para*-chloro substituent, showed a considerable increase in potency, with an IC₅₀ of 64.2 nM toward PHD2; this made it the most active compound among them almost nine-times more active than clinical drug **1**. The introduction of a weak electron-donating methyl group (**18-20**) seemed to be beneficial for activity; the IC₅₀ values of these compounds ranged from 70.4 nM to 125 nM, showing improved potency as compared to **8**. However, introducing a strong electron-withdrawing trimethyl group (**21-23**) resulted in great loss in potency, with IC₅₀ values ranging from 514 nM to 1073 nM. Methoxy-substituted compounds (**24-26**) were found to have slightly decreased inhibitory activity as compared to **8**. In addition, *para*-substitutions with ethyl (**27**), cyano (**28**), and phenyl (**29**) were all detrimental for PHD2 inhibition. Notably, **29**, with a bulky phenyl substitution, was much less active than **8**. Moreover, replacing phenyl in **8** with a naphthyl group as in **30** caused about a two-fold decrease in potency. The above results suggest that a strong electron-withdrawing or steric moiety around the phenyl group of **8** is unfavorable and *para*-chloro substitution, as in **17**,

contributes greatly to the compound's inhibitory activity. However, further introduction of another chloro group, as in **31** and **32**, resulted in decreased potency as compared to **17**. Furthermore, bringing a methylene link between the phenyl and oxygen atom (**33**) retained its activity, while further extending to a two-atom linker (**34**) led to a significant loss in potency as compared to **17**.

Table 2. SAR on the phenyl group of **8**



compound	n	R	PHD2 IC ₅₀
12	0	2-F	444 ± 24
13	0	3-F	256 ± 4
14	0	4-F	186 ± 8
15	0	2-Cl	175 ± 3
16	0	3-Cl	587 ± 22
17	0	4-Cl	64.2 ± 1.1
18	0	2-Me	70.4 ± 0.6
19	0	3-Me	125 ± 5
20	0	4-Me	110 ± 2
21	0	2-CF ₃	1073 ± 8
22	0	3-CF ₃	877 ± 5
23	0	4-CF ₃	514 ± 6
24	0	2-MeO	218 ± 21
25	0	3-MeO	428 ± 3
26	0	4-MeO	186 ± 4
27	0	4-Et	378 ± 33
28	0	4-CN	263 ± 15
29	0	4-Ph	825 ± 3
30	0	-	346 ± 1
31	0	2,4-di-Cl	450 ± 20
32	0	3,4-di-Cl	527 ± 6
33	1	4-Cl	84.3±12.7

1				
2				
3	34	2	4-Cl	408 ± 7
4	8	0	H	169 ± 1
5	FG-4592 (1)			591 ± 13
6	<hr/>			
7				
8				
9				

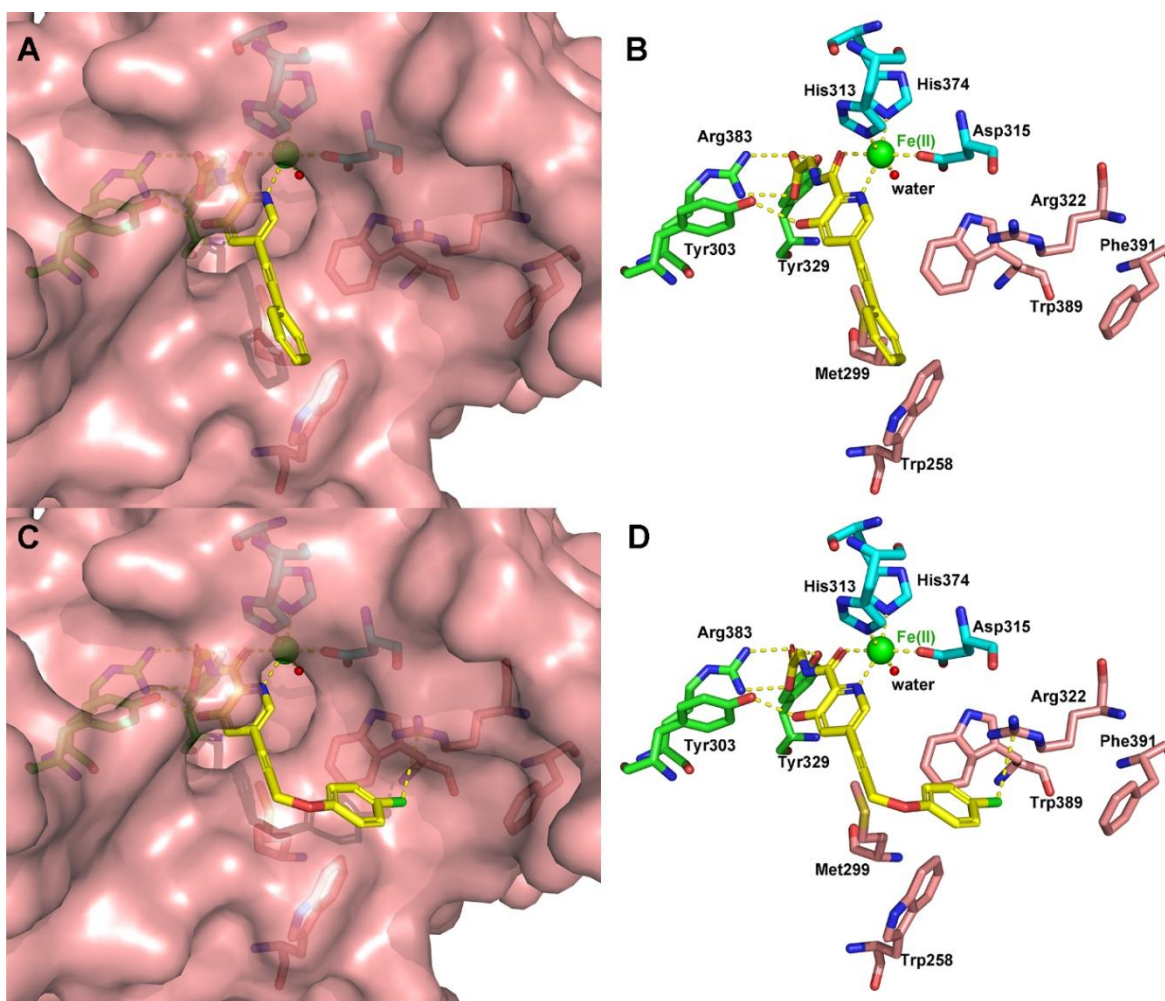
2.2. Molecular modeling.

To obtain deeper insight into the critical structural features of the binding mode between these alkynyl compounds and the PHD2 enzyme, molecular docking studies were performed utilizing the protein ligand docking software GOLD 5.1 for representative compounds **6** and **17**. The optimizing settings for docking procedures were established using the X-ray crystallographic structure of a complex of wild-type PHD2 and an **FG-2216**-like inhibitor (PDB ID: 2G19; Figure S1).¹⁷ Docking poses were analyzed using the visualization program PyMOL 2.3.0.

The binding mode of **6** with PHD2 was firstly analyzed by docking (Figure 2A). The results showed that the pyridine nitrogen atom and the amide oxygen atom formed a 5-membered ring with Fe(II) that was coordinated by the residues of His313, Asp315, and His375, together with water, generating an octahedral structure. The terminal carboxy of the glycine moiety could form an interaction network with the Tyr329 and Arg383 residues through hydrogen-bonding and electrostatic interactions, respectively. Additionally, the phenolic hydroxyl of **6** showed hydrogen-bonding with Tyr303 and the phenyl extending to the solvent area exhibited an orthogonal π - π stacking with Trp258.

To understand the reason why a minor change in structure led to such a great increase in potency, we compared the docked poses of **17** and the less active **6** into the PHD2 binding sties (2G19). As shown in Figure 2, the docking poses of **6** and **17** possessed a critical chelating interaction with Fe (II), an interaction network with Arg383 and Tyr329, and a hydrogen-bonding

1
2
3 interaction with Tyr303. In contrast to **6**, the phenyl of **17** was capable of forming an additional
4 potential interaction with a pocket formed by the residues of Arg322, Trp389, Trp258, and Phe391.
5
6 T-shaped π - π stacking interactions between Trp258, Trp389, and the phenyl of **17** were present.
7
8 In addition, a cation- π interaction between the phenyl of **17** and Arg322 was observed. Further,
9
10 the 4-substituted chlorine atom on the phenyl retained a hydrogen-bonding interaction with the
11 positive center of Arg322; this may lead to a strong synergistic effect in enhancing the interaction
12 between phenyl and Arg322. This effect can explain, to some extent, why 4-substituted chlorine
13 plays a significant role in the remarkable increase in inhibitory activity toward PHD2.
14
15
16
17
18
19
20
21
22

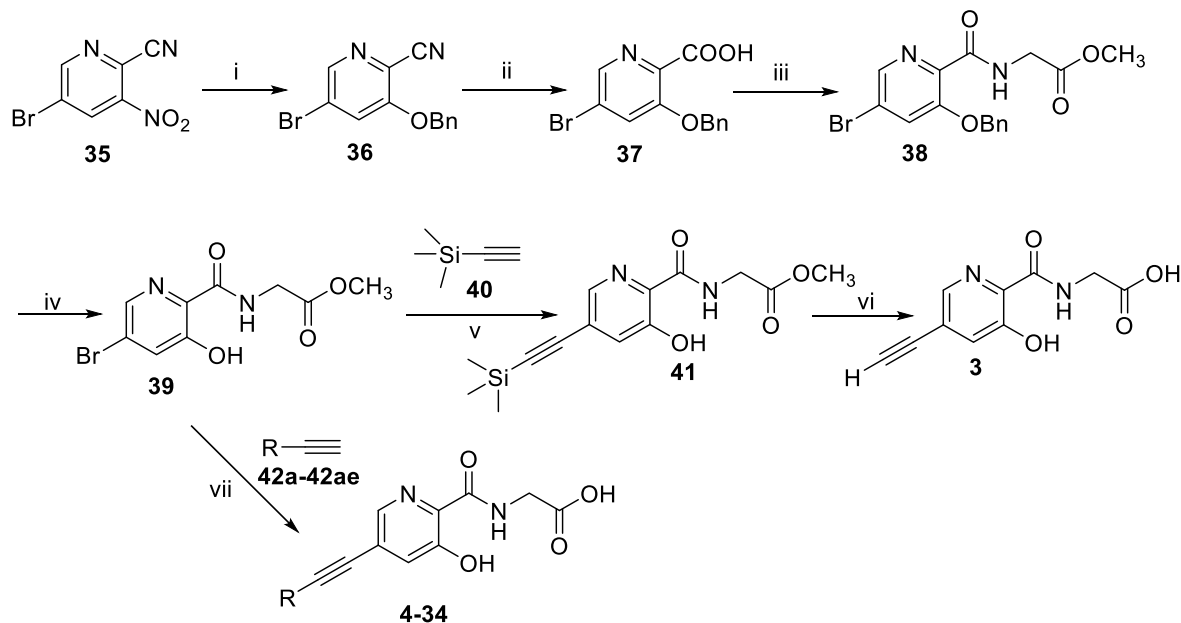


1
2
3 **Figure 2.** Proposed binding modes: structure of **6** and **17** docked into PHD2 (PDB ID 2G19). A,
4 B (**6**, yellow carbons), C, D (**17**, yellow carbons) in the PHD2 active site. The key interactions
5
6 between inhibitors and PHD2 are depicted as yellow dashes.
7
8
9

10 11 **2.3. Synthesis of target compounds 3-34.**

12
13
14 The synthetic route of target compounds **3-34** is depicted in **Scheme 1**. The key intermediate, **38**,
15 was obtained from starting material **35**, according to the method reported previously.²⁹ The nitro
16 group of **35** was substituted with benzyl alcohol under the strong base condition to give **36**.
17 Subsequent hydrolysis of the cyano group of **36** in the presence of 30% aqueous NaOH yielded
18 the carboxylic acid, **37**. The condensation reaction between **37** and GlyOMe·HCl was applied in
19 the presence of EDC·HCl and HOBT to obtain the key intermediate, **38**. Following that reaction,
20
21 **38** was treated with BF₃·Et₂O to give **39**, which was coupled with trimethylsilylacetylene (**40**)
22 using Pd(PPh₃)₂Cl₂ and CuI as the catalysts under microwave irradiation condition to yield **41**.
23 Target compound **3** was obtained by deprotection of trimethylsilyl using tetrabutylammonium
24 fluoride (TBAF) followed by hydrolysis of the methyl ester. Further, **39** was treated with different
25 ethynyl fragments (**42a-42ae**) under a Sonogashira reaction followed by hydrolysis of the methyl
26 group, yielding the desired alkynyl-containing PHD2 inhibitors (**4-34**).
27
28
29
30
31
32
33
34
35
36
37
38
39
40
41

42 **Scheme 1** ^a



^a Reagents and conditions: (i) BnOH, NaH, THF, rt to 35 °C, 1.5 h, 86.7%; (ii) NaOH, CH₃OH, H₂O, reflux, 2 h, 86.8%; (iii) GlyOMe·HCl, TEA, HOBT, EDCI, DCM, rt, 6 h, 46.5%; (vi) BF₃·Et₂O, DCM, 45 °C, 6 h, 73.5%; (v) Pd(PPh₃)₂Cl₂, CuI, Et₃N, CH₃CN, microwave irradiation, 120 °C, 300W, 7 min, 90.0%; (vi) TBAF, MeOH, reflux, 1h; then, LiOH, THF, H₂O, 35 °C, 1 h, 84.1% over two steps; (vii) Pd(PPh₃)₂Cl₂, CuI, DIPEA, DMF, microwave 120 °C, 300 W, 15 min; then, LiOH, THF, H₂O, 35 °C, 1h, 31.0–82.3% over two steps.

2.4. Selectivity of alkynyl compounds represented by 17 to other PHD subtypes, 2-OG oxygenases, and hERG.

To investigate whether the alkynyl-containing PHD2 inhibitor (**17**) selectively inhibited PHD2, its potency against other PHD subtypes (PHD1, PHD3) and representative 2-OG oxygenases, such as JmjC-domain-containing lysine histone demethylases (KDMs), were determined by *O*-phenylenediamine (OPD)-based fluorescent assay (Table S1)³⁰ and AlphaScreen assay (Table S2),¹⁹ respectively. The results indicated that **17** also showed significant PHD3 inhibitory activity ($SR_{(PHD3)} = 2.6$) and exhibited considerable selectivity to the PHD1 subtype ($SR_{(PHD1)} = 29$) (Table

3). The subtype selectivity of **17** is similar to that of the approved drug **FG-4592**, thus, alkynyl-containing PHD2 inhibitors can modulate the HIF pathway, mainly by inhibiting PHD2 and PHD3, thereby efficiently stabilizing HIF- α . Moreover, the AlphaScreen assay demonstrated that **17** retains 156-fold more selectivity for PHD2 over typical JmjC-KDMs such as KDM3A, KDM4A, and KDM6B (Table 3). To verify whether **17** has the potential for cardiac toxicity, a hERG assay³¹ was performed. No hERG inhibition was observed for **17**, which showed a 467-fold selectivity to PHD2 over hERG (Tables 3 and S3). These enzyme-based results indicate that **17** is a promising PHD inhibitor with good selectivity windows for HIF stabilization.

Table 3. Selectivity Ratio of the Representative Compound to PHD2 Over PHD1, PHD3, JmjC-KDMs, and hERG

compound	SR _(PHD1) ^a	SR _(PHD3) ^a	SR _(KDM3A) ^b	SR _(KDM4A) ^b	SR _(KDM6B) ^b	SR _(hERG) ^c
17	29	2.6	>1556	1556	>156	>467
FG-4592 (1)	5.0	1.1	>169	169	>169	ND ^d

^a SR = IC₅₀ (PHDs)/IC₅₀ (PHD2). The SR was generated using the IC₅₀ values towards PHDs determined by OPD assay. ^b SR = IC₅₀ (JmjC-KDMs) / IC₅₀ (PHD2). The SR was generated using the IC₅₀ values towards PHD2 determined by FP assay and towards typical JmjC-KDMs determined by AlphaScreen assay. ^c SR = IC₅₀ (hERG)/IC₅₀ (PHD2). The SR was generated using the IC₅₀ values towards PHD2 determined by FP assay and those towards hERG determined by hERG patchliner assay. ^d Not determined.

2.5. Representative compound **17** stabilized HIF- α and upregulated the expression and secretion of EPO.

To validate the HIF- α stabilization effect of **17**, the immunostaining method was performed to visualize changes in **17**-treated Hep3B cells. The results demonstrated that **17** and **FG-4592** up-

1
2
3 regulated the levels of HIF- α subunits, both HIF-1 α and HIF-2 α , in a dose-dependent manner
4 (Figure 5A). Considering that HIF can consequently bind to the hypoxia-responsive element (HRE)
5 motif on DNA, thereby promoting the expression of EPO, we used an HRE-luciferase dual-
6 reporter assay to further validate the stabilizing effect of **17** to HIF- α .³² Before that, a 3-(4, 5-
7 dimethylthiazol-2-yl)-2,5-diphenyltetrazolium bromide (MTT) assay was conducted to investigate
8 whether **17** kills typical normal cells and experimental cells; no lethal effect of **17** was observed
9 towards these typical cells, indicating it has a good cell-based safety profile (Figure S2). As shown
10 in Figure 3B, **17** exhibited stabilization activity for HIF- α comparable to **FG-4592**; the HIF- α level
11 was upregulated four-fold with the treatment of 25 μ M **17** and seven-fold with 50 μ M **17**.
12
13
14
15
16
17
18
19
20
21
22
23

24
25 To further confirm the effects of **17** on the EPO gene, RT-PCR was used to evaluate the
26 mRNA level of the EPO gene. Treatment of Hep3B cells with **17** dose-dependently upregulated
27 the EPO mRNA level in Hep3B cells, showing an approximate seven-fold upregulation with a
28 concentration of 50 μ M (Figure 3C). Subsequently, we examined the level of EPO production to
29 further reveal the potency of **17** in regulating the HIF pathway. EPO ELISA assay revealed that
30 **17** was capable of significantly improving EPO expression in a dose-dependent manner in Hep3B
31 cells (Figure 3D). Based on these results, the PHD inhibitor **17** exhibits remarkable efficacy in
32 stabilizing HIF- α , leading to the promotion of EPO expression.
33
34
35
36
37
38
39
40
41
42
43
44
45
46
47
48
49
50
51
52
53
54
55
56
57
58
59
60

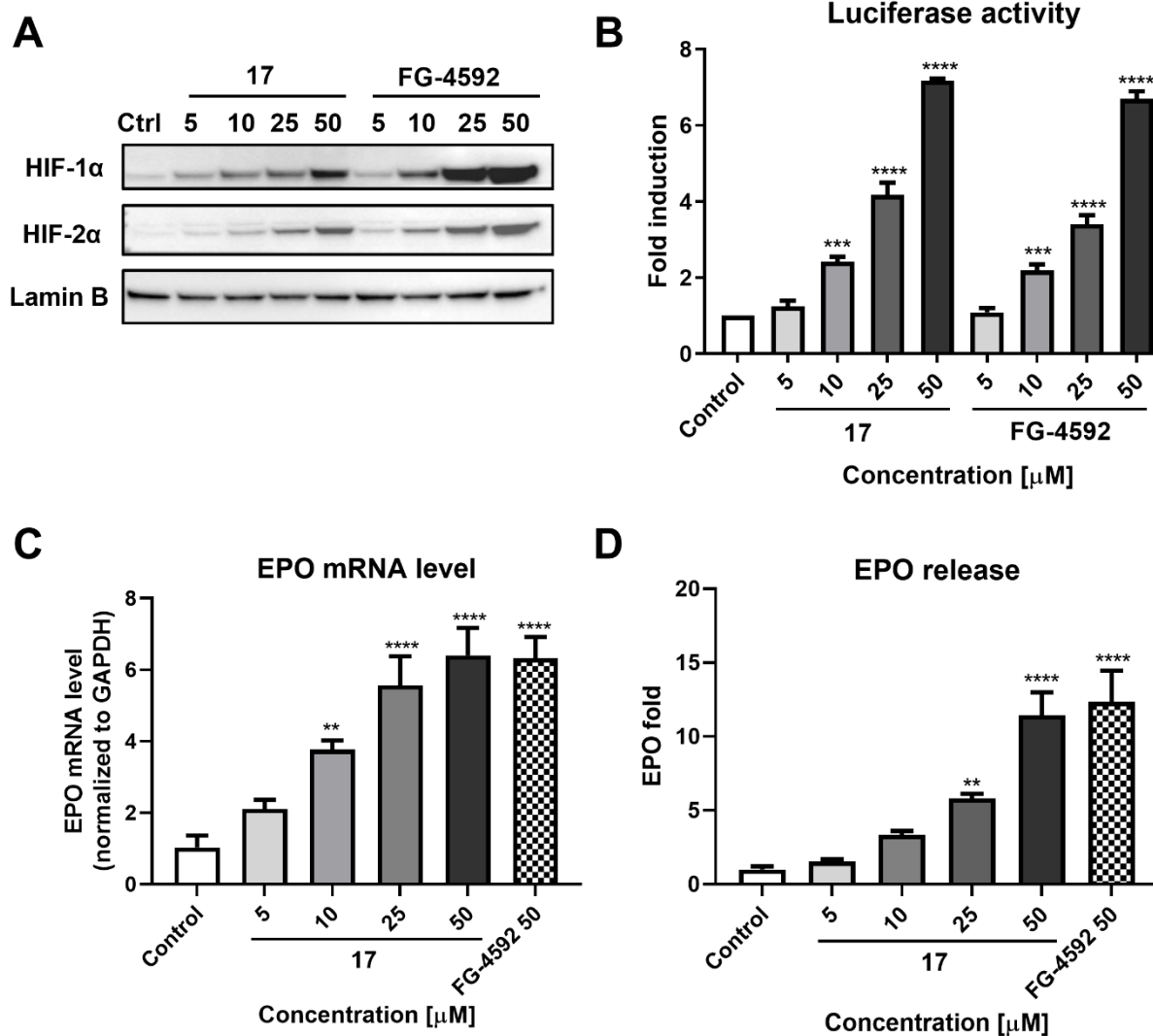


Figure 3. Evaluation of the potency of **17** in HIF- α stabilization and EPO upregulation. (A) Representative western blot visualization of HIF- α levels in **17**-treated Hep3B cells; Lamin B was used as the control for HIF- α loading. (B) Expression of HIF target genes after treatment MCF-7 cells with **17**. (C) Expression of EPO genes in Hep3B cells by RT-PCR after incubation with **17** for 10 h. (D) EPO release in **17**-treated Hep3B cells after 24 h. P values were analyzed by two-way ANOVA with the control group as the comparison (*, $P < 0.05$; **, $P < 0.01$; ***, $P < 0.001$; ****, $P < 0.0001$).

2.6. Evaluation of the effects of representative compounds on the plasma EPO levels *in vivo*.

Inspired by the PHD2 inhibition activity *in vitro*, *in vivo* pharmacodynamic (PD) evaluation in mice was carried out. In light of their potency of PHD2 inhibition, nine representative compounds (8, 14, 15, 17, 18, 19, 20, 26, and 33) with IC₅₀ values less than 200 nM toward PHD2, together with the approved drug FG-4592, were selected. C57BL/6 mice were treated with each compound at a dose of 15 mg/kg via *iv* administration. Then, the levels of plasma EPO were investigated using an EPO-based ELISA Kit.^{33,34} As shown in Figure 4A, compounds 15, 17, 19, and 26 exerted obvious EPO upregulation at more than 1000 pg/mL. Further, the pharmacodynamics of the four effective compounds were evaluated with *po* administration in C57BL/6 mice at 15 mg/kg. The results indicated that 17 produced the best upregulation of the plasma EPO levels; its effect was even better than the positive control FG-4592 (Figure 4B).

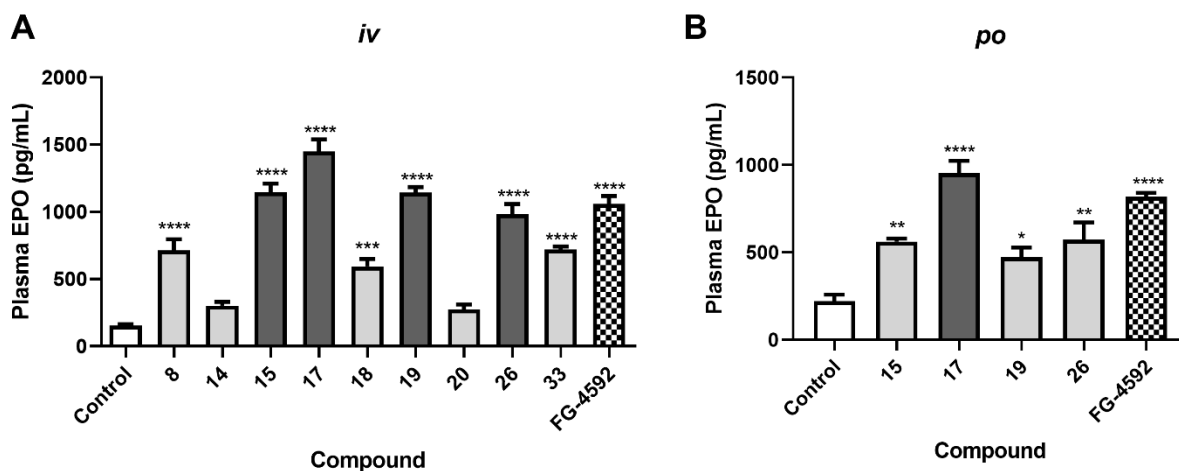


Figure 4. *In vivo* upregulation of EPO. (A) Plasma EPO levels in mice (C57BL/6) treated with 15mg/kg of each compound; levels were tested 4 h after *iv* administration. (B) The typical compounds (15mg/kg) produced plasma EPO responses in mice (C57BL/6) 4 h after *po*

1
2
3 administration. Mean \pm SEM. P values were analyzed by two-way ANOVA with the control group
4 as the comparison (*, P < 0.05; **, P < 0.01; ***, P < 0.001; ****, P < 0.0001).
5
6
7

8 **2.7. Compound 17 dose-dependently increases the plasma EPO and reticulocytes *in vivo*.**

9
10 Dose-dependent PD assays for EPO induction in mice were further conducted for **17** and **FG-**
11 **4592**.²³ Increases in plasma EPO were observed at 5, 10, 25, and 50 mg/kg, with doses given four
12 times for three consecutive days by *po* administration (Figure 5). Notably, stabilization of HIF by
13 *po* administration of **17** resulted in dose-dependent elevation of plasma EPO levels in C57BL/6
14 mice, which was similar to the **FG-4592**-treated group. Interestingly, in the case of the 25 mg/kg
15 dosage, **17** was more efficacious in the upregulation of plasma EPO as compared to FG-4592. The
16 effects on reticulocyte generation were also evaluated. After 72 h (*po* administration of the
17 compound three times) of treatment with **17** or **FG-4592**, RBC% (the reticulocyte count/the red
18 blood cell count) increased under both treatments in a dose-dependent manner (Figure 6). These
19 results suggest that the orally-active PHD inhibitor **17** upregulates EPO formation and stimulates
20 erythropoiesis.
21
22
23
24
25
26
27
28
29
30
31
32
33
34
35
36
37
38
39
40
41
42
43
44
45
46
47
48
49
50
51
52
53
54
55
56
57
58
59
60

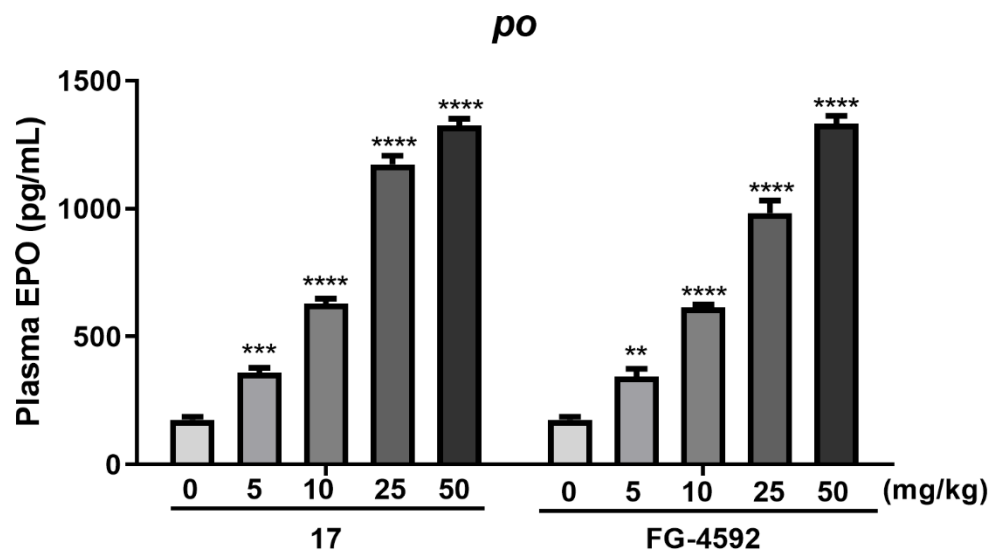


Figure 5. 17- and FG-4592-mediated plasma EPO response in mice (C57BL/6) after three days of *po* administration of each compound (5, 10, 25, and 50 mg/kg). Mean \pm SEM. P values were analyzed by two-way ANOVA with the control group as the comparison (*, $P < 0.05$; **, $P < 0.01$; ***, $P < 0.001$; ****, $P < 0.0001$).

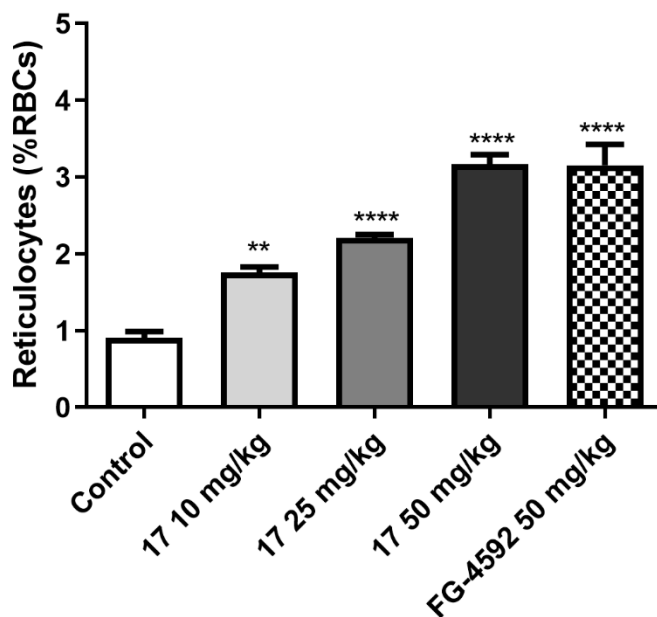


Figure 6. Reticulocytes (RBC %) were measured 72 h (after *po* administration of each compound three times) after treatment with **17** or **FG-4592**. Mean \pm SEM. P values were analyzed by two-way ANOVA with the control group as the comparison (*, $P < 0.05$; **, $P < 0.01$; ***, $P < 0.001$; ****, $P < 0.0001$).

2.8. Pharmacokinetic and metabolic profiles of **17**.

Pharmacokinetic studies of **17** in healthy rats and beagle dogs were performed to evaluate absorption, distribution, metabolism, and excretion (ADME) properties. As shown in Table 4, **17** exhibited acceptable $T_{1/2}$ in rats (6.44 ± 3.08 h) and beagle dogs (4.19 ± 1.98 h) with *ig* administration. Suitable bioavailability was observed both in rats (55.7%) and beagle dogs (55.4%), verifying the potential application of this compound for further research *in vivo*. In addition, the *in vitro* metabolic stability of **17** was assessed in liver microsomes from different species (Table 5). The results showed that **17** possessed suitable stability in these five liver microsomes, especially in human microsomes. The metabolic stability of **17** was further assessed in rat/mice hepatocytes and human L02 cells; the metabolism of **17** in human L02 cells seemed to be much slower than in mice and rat hepatocytes (Table 6), suggesting that **17** may possess suitable pharmacokinetic behavior with superior stability in humans. **17** was assayed with cytochrome p450 (CYP450) enzymes; no significant inhibition *in vitro* was observed toward CYP450 enzyme isomers, including CYP1A2, 2C1, 2C9, 2D6, and 3A4, with all IC_{50} values above 30 μ M (Table 7); this suggests the low potential for **17** to produce clinical drug-drug interactions.

Table 4. Pharmacokinetic Profiles of **17** in Rats and Beagle Dogs.^a

	rat (<i>ig</i> , 2 mg/kg)	rat (<i>iv</i> , 1 mg/kg)	dog (<i>ig</i> , 2 mg/kg)	dog (<i>iv</i> , 0.5 mg/kg)
--	----------------------------	----------------------------	----------------------------	------------------------------

T_{\max} (h)	0.63 ± 0.25	—	0.67 ± 0.29	—
C_{\max} (ng/mL)	1027 ± 374	—	735 ± 493	—
AUC_{0-t} (ng/ml*h)	4795 ± 2150	4709 ± 346	1357 ± 329	611 ± 67
$AUC_{0-\infty}$ (ng/ml*h)	5418 ± 2517	4864 ± 337	1374 ± 343	636 ± 58.3
$T_{1/2}$ (h)	6.44 ± 3.08	8.43 ± 1.70	4.19 ± 1.98	2.91 ± 1.11
CL (mL/min/kg)	7.30 ± 3.34	3.44 ± 0.23	25.5 ± 7.3	13.2 ± 1.3
V_z (mL/kg)	3409 ± 434	2515 ± 540	8417 ± 2535	3340 ± 1305
$MRT_{0-\infty}$ (h)	9.43 ± 2.62	3.44 ± 0.55	4.69 ± 1.07	2.27 ± 0.69
F	55.7%		54.0%	

^a For rats, N = 4; equal number of males and females; for dogs, N = 3, all males.

Table 5. *In Vitro* Metabolic Stability of **17** in Liver Microsomes.

liver microsome	mouse	rat	dog	monkey	human
CL_{int} ($\mu\text{L}/\text{min}/\text{mg}$)	<10.00	<20.00	<10.00	<13.00	<10.00
CL (mL/min/kg)	<27.00	<26.00	<9.60	<13.00	<6.30
$T_{1/2}$ (min)	>139.00	>67.00	>139.00	>99.00	>139.00

Table 6. *In Vitro* Metabolic Stability of **17** in Rat/Mice Hepatocytes and Human L02 Cells.

hepatocyte	mouse	rat	human
CL (mL/min/kg)	82.16	35.62	1.54

T _{1/2} (min)	8.68	32.3	1062.7
---------------------------	------	------	--------

Table 7. Inhibition of Cytochrome P450 (CYP450) Enzymes by **17**.

isozyme ^a	IC ₅₀ (μM)
CYP1A2 (phenacetin)	>30
CYP2C1 (9-(S)-mephenyt)	>30
CYP2C9 (diclofenac)	>30
CYP2D6 (dextromet horphan)	>30
CYP3A4 (testosterone)	>30
CYP3A4 (midazolam)	>30

^a CYP450 isozymes and the corresponding substrate drugs.

2.9. Oral administration of **17** improves cisplatin-induced anemia.

Encouraged by its promising *in vivo* pharmacodynamic (PD) and pharmacokinetic (PK) properties, **17** was further assessed in a cisplatin-induced anemia C57BL/6 mouse model to evaluate its anti-anemia efficacy.³⁵ The hemoglobin (Hb) level in the cisplatin-administered mice was decreased to 130 g/L as compared with the normal control. In the male mice model, **17** and **FG-4592** treatment at dosages of 10 and 25 mg/kg every other day for 30 days produced a dose-dependent increase in Hb levels. Similar to **FG-4592**, treatment with **17** prevented the development of anemia induced by cisplatin; plasma Hb levels under **17** treatment recovered to levels observed without cisplatin stimulation (Figure 7A). Interestingly, **17** was found to restore Hb to normal levels while **FG-4592** caused a slight shift to above the normal level (Figure 7B), indicating that **17** may possess a preferable safety profile for anemia treatment, particularly at high doses for long periods of time.

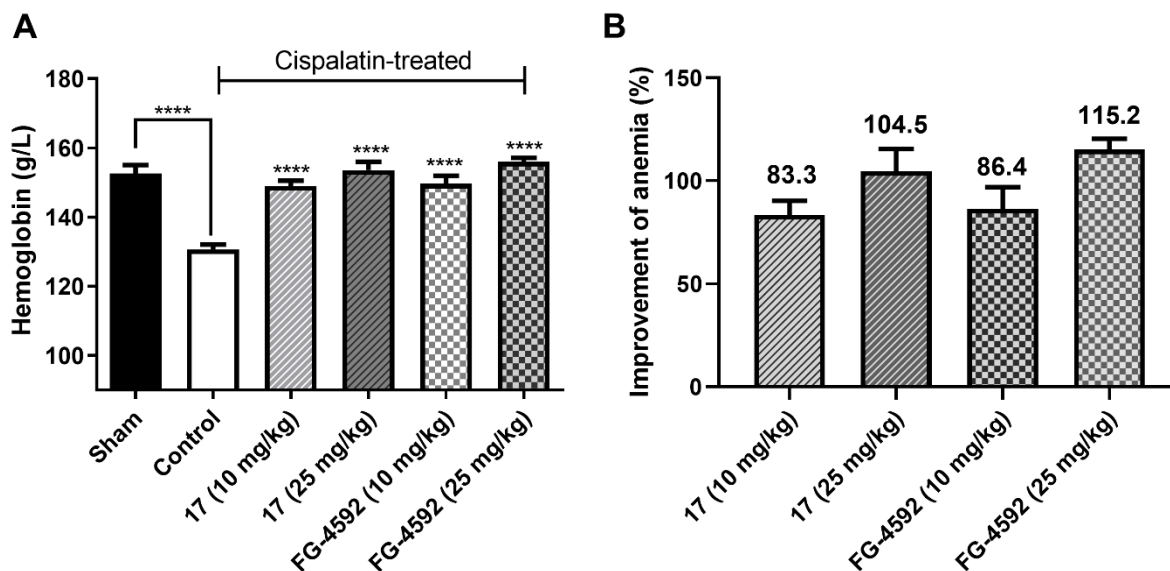


Figure 7. Anti-anemia potential *in vivo*. (A) Changes in Hb after oral administration of **17** or **FG-4592** in a C57Bl/6 mouse model of anemia induced by cisplatin. (B) Anti-anemia activities of **17** or **FG-4592** in a C57Bl/6 mouse model of anemia induced by cisplatin. Mean \pm SEM. P values were analyzed by two-way ANOVA with the control group as the comparison (*, $P < 0.05$; **, $P < 0.01$; ***, $P < 0.001$; ****, $P < 0.0001$).

2.10. Subacute toxicity and genetic safety assessment of **17**.

To further evaluate its *in vivo* safety profile, the acute toxicity of **17** was determined in SD rats at doses of 15, 50, and 200 mg/kg. The treatment period involved *iv* administration of **17** for two weeks. During this time, none of the animals showed any abnormal behavior as compared to the no-treatment group. During the 14 days of treatment, food intake, body weight, and organ/body weight ratios were recorded (Figure 8). It was observed that body weights and food intake were relatively stable and the growth trend was consistent with the blank control. Furthermore, no obvious changes were observed after **17** treatment with respect to the organ/body weight ratio of

1
2
3 the adrenal gland, brain, heart, kidney, liver, thymus, thymus, ovary (female), uterus with cervix
4 (female), testes (male), and epididymis (male); however, a slight increase in the weight of the
5 spleen (male) occurred which may be ascribed to the pharmacological effect of the compound
6 along with the elevation of EPO levels.³⁶ Additionally, blood biochemistry studies revealed that
7
8 **17** had no obvious nephrotoxicity and hepatotoxicity in SD rats compared to the control group
9 (Figure 9), as determined by kidney function indicators (urea; CRE, creatinine) and liver function
10 indicators (AST, aspartate aminotransferase; ALT, alanine amiotransferase; A/G, albumin/
11 globulin; GLO, globulin; ALB, albumin; TP, total protein). Only a slight increase in AST was
12 observed at a dosage of 200 mg/kg in male rats (Figure 9F). The above results indicate that **17** has
13 a preferable safety profile with no acute toxicity to normal tissues and a wide therapeutic window.
14
15 Moreover, the genotoxicity of **17** was also evaluated by AMES assay and no significant
16 genotoxicity of **17** was observed (Table S4). Taken together, these findings indicate that **17** has an
17 acceptable safety profile *in vivo* and is suitable for further clinical development.
18
19
20
21
22
23
24
25
26
27
28
29
30
31
32
33
34
35
36
37
38
39
40
41
42
43
44
45
46
47
48
49
50
51
52
53
54
55
56
57
58
59
60

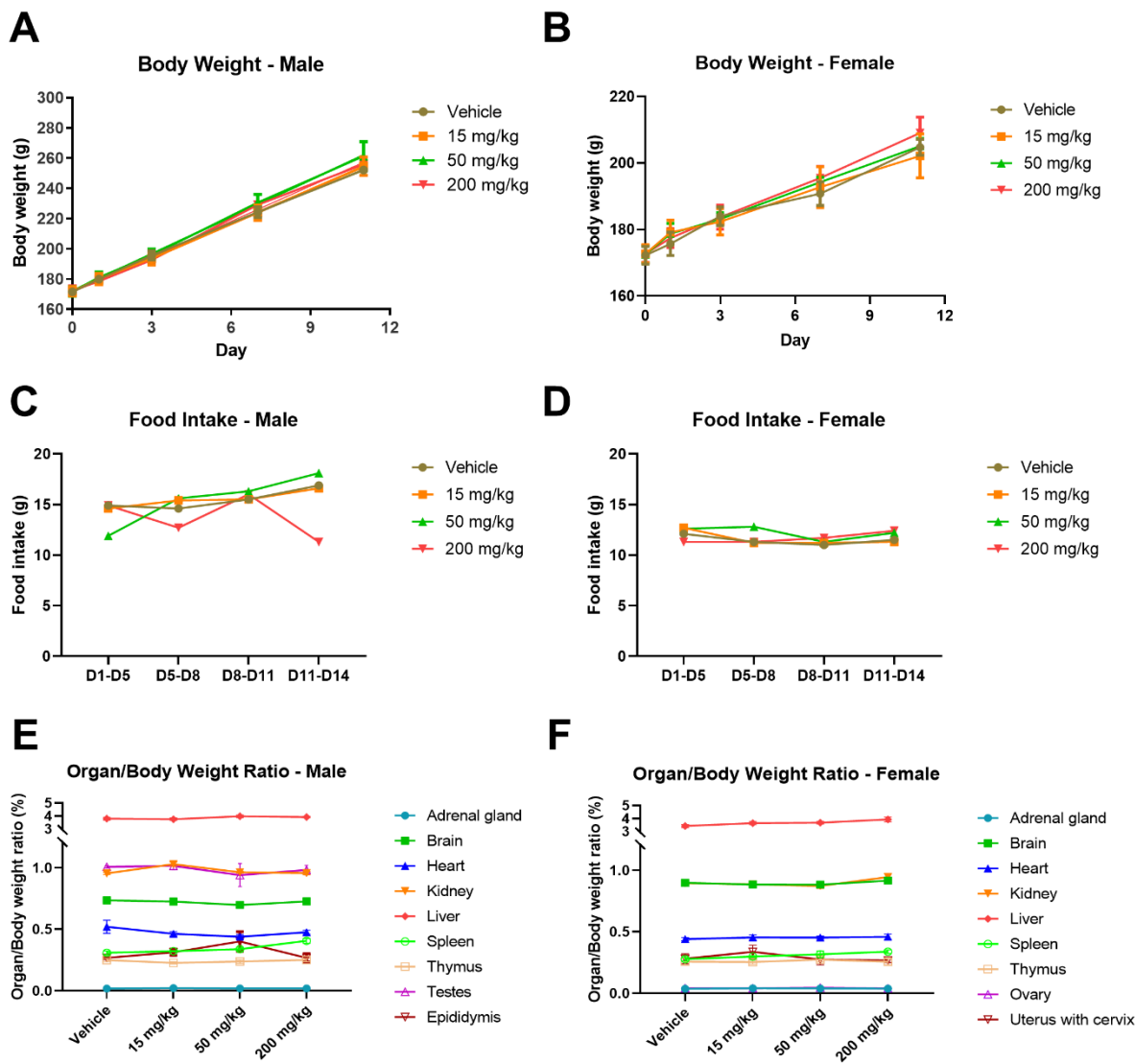


Figure 8. The effects of compound **17** on body weight (A/B), food intake (C/D), and organ/body weight ratio (E/F) in rats (*iv*; 15, 50, and 200 mg/kg). (A) Changes in bodyweight (male rats); (B) changes in bodyweight (female rats); (C) changes in food intake (male rats); (D) changes in food intake (female rats); (E) changes in organ/body weight ratio (male rats); (F) changes in organ/body weight ratio (female rats).

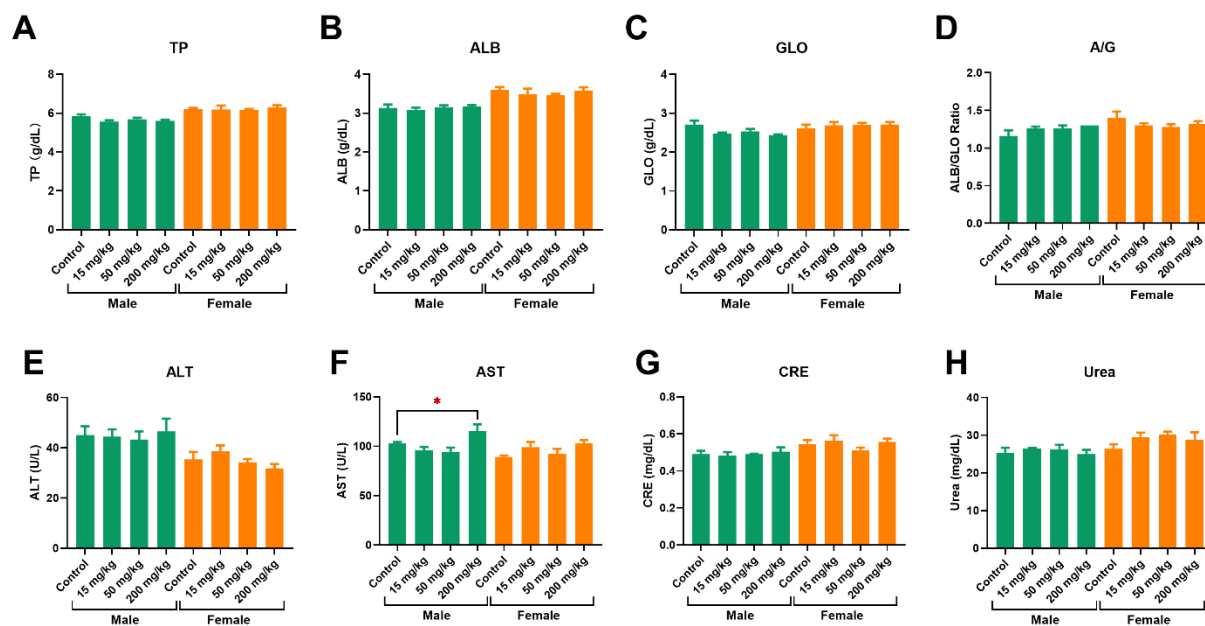


Figure 9. Blood biochemistry analysis of TP, ALB, GLO, A/G, ALT, AST, CRE, and urea indicators in rats. Mean \pm SEM. P values were analyzed by two-way ANOVA with the control group as the comparison (*, $P < 0.05$).

3. CONCLUSION

In this work, we developed a novel series of alkynyl-containing PHD inhibitors by replacing the rigid isoquinoline core in **FG-4592** with a rigid and linear 5-alkynyl pyridine core. Of these, **17** was identified as the most active compound both *in vitro* and *in vivo*. On the basis of its overall pharmacological, pharmacokinetic, and preliminary safety profile, **17** has been advanced to human clinical studies as an oral treatment for anemia.

4. EXPERIMENTAL SECTION

4.1. General Methods and Materials. All materials were purchased from commercial sources and used as received. Organic solvents were concentrated via a rotary evaporator (EYELA OBS-

2100) under reduced pressure below 50 °C. The microwave reactions were performed on a microwave reactor from Biotage, Inc. Reactions were monitored using TLC silica gel plates (GF254, 0.25 mm) and visualized under UV light. Hanon MP420 automatic melting point apparatus was used to determine the melting points. The Proton nuclear magnetic resonance (¹H NMR) and carbon nuclear magnetic resonance (¹³C NMR) spectra were determined using Bruker AV-300 instruments. EI-mass spectra and high-resolution mass spectra (HRMS) were recorded on a Shimadzu GCMS-2010 mass spectrometer and a Water Q-ToF micro mass spectrometer, respectively. The purity (≥95%) of the target compounds used for biological testing were evaluated by high-performance liquid chromatography (HPLC) analysis, performed on an Amethyst C18-P (4.6 × 150 mm, 5 μM, Merck) column eluting with methanol/water (80:20 v:v) containing 0.1% trifluoroacetic acid at a flow rate of 0.5 mL/min; the peaks were detected at 254 nm under UV. The experimental cells were purchased from Cell Bank of Shanghai, Institute of Biochemistry and Cell Biology, Chinese Academy of Sciences. FITC-HIF-1α (556-574) was purchased from Shanghai Apeptide Co., Ltd., the typical proteins from Nanjing Zoombio biotechnology, and the experimental mice were obtained from Beijing Vital River Laboratory Animal Technology Co., Ltd. All animal-related experiments were conducted under a China Pharmaceutical University IACUC approved protocol (No. 20160622-1) in compliance with the guide for the care and use of laboratory animals.

4.2. Synthesis. 4.2.1. Preparation of 3-(Benzyloxy)-5-bromopicolinonitrile (36). A solution of benzyl alcohol (59 mL, 570 mmol) in THF (1.8 L) was cooled to 0 °C. NaH (14.4 g, 600 mmol) was added slowly to the stirring mixture at 0 °C. Then, the mixture was stirred at room temperature for 1 h and at 35 °C for another 0.5 h. The resulting solution was added to a solution of 5-bromo-3-nitropicolonitrile (**35**, 100.0 g, 438 mmol) in THF (1.3 L) and then the mixture was stirred at

1
2
3 room temperature for 24 h. The reaction mixture was quenched with H₂O (200 mL), and
4 concentrated to a volume of about 200 mL. DCM (1.5 L) was added. The organic layer was
5 separated, washed with saturated NaHCO₃ solution (1.0 L × 1), water (1.0 L × 2), and saturated
6 brine (1.0 L × 1). The organic layer was concentrated and dried under vacuum at 55 °C to afford the
7 brown solid **36** (110.0 g, 86.7%). mp 116.5–119.0 °C. ¹H NMR (300 MHz, CDCl₃) δ 5.26 (s, 2H),
8 7.36–7.48 (m, 5H), 7.56 (d, *J* = 1.5 Hz, 1H), 8.35 (s, 1H); HRMS (ESI): calcd. for C₁₃H₉BrN₂O
9 [M + H]⁺ 288.9972 and 290.9951, found 288.9970 and 290.9952.

10
11
12 **4.2.2. Preparation of 3-(Benzyloxy)-5-bromopicolinic acid (37).** A suspension of **36** (53.3 g,
13 184 mmol), methanol (1.0 L) and 30% NaOH (1.0 L) was refluxed for 2 h. The mixture was cooled
14 to room temperature and concentrated to a volume of about 1.0 L. The resulting mixture was
15 acidified by 10% HCl aqueous solution to pH = 2. The precipitate was collected, washed with
16 water, and dried to afford the pale yellow solid **38** (49.3 g, 86.8%). mp 93.3–95.5 °C. ¹H NMR
17 (300 MHz, CDCl₃) δ 5.32 (s, 2H), 7.27–7.36 (m, 3H), 7.38–7.45 (m, 2H), 7.67 (s, 1H), 8.29 (s,
18 1H). HRMS (ESI): calcd. for C₁₃H₁₀BrNO₃ [M + H]⁺ 307.9917 and 309.9897, found 307.9913 and
19 309.9900.

20
21
22 **4.2.3. Preparation of Methyl (3-(benzyloxy)-5-bromopicolinoyl)glycinate (38).** To a solution
23 of **37** (49.3 g, 0.16 mol) in DCM (500 mL) was added Et₃N (67 mL, 0.48 mol), HOBT (32.4 g,
24 0.24 mol), EDCI (46.0 g, 0.24 mol), and glycine methyl ester hydrochloride (24.1 g, 0.192 mol).
25 The mixture was stirred at room temperature for 6 h. Saturated NaHCO₃ solution (1.0 L) was then
26 added and the aqueous layer removed. The organic layer was washed with water (1.0 L × 2) and
27 saturated brine (1.0 L × 3), dried over anhydrous MgSO₄, filtrated and concentrated. The residue
28 was recrystallized from petroleum ether: EtOAc = 3:1 to afford the white solid **38** (28.2 g, 46.5%).
29 mp 101.2 – 102.9 °C. ¹H NMR (300 MHz, CDCl₃) δ 3.79 (s, 3H), 4.27 (d, *J* = 5.4 Hz, 2H), 5.26
30
31
32
33
34
35
36
37
38
39
40
41
42
43
44
45
46
47
48
49
50
51
52
53
54
55
56
57
58
59
60

(s, 2H), 7.25–7.44 (m, 3H), 7.52 (d, $J = 7.5$ Hz, 2H), 7.58 (d, $J = 1.5$ Hz, 1H), 8.17 (s, 1H), 8.31 (d, $J = 1.5$ Hz, 1H). ^{13}C NMR (75 MHz, CDCl_3) δ 40.79, 51.86, 70.82, 123.15, 124.81, 126.60, 127.86, 128.33, 134.56, 136.68, 141.11, 154.50, 162.90, 169.78. HRMS (ESI): calcd. for $\text{C}_{16}\text{H}_{15}\text{BrN}_2\text{O}_4$ $[\text{M} + \text{H}]^+$ 379.0288 and 381.0268, found 379.0294 and 381.0275.

4.2.4. Preparation of Methyl (5-bromo-3-hydroxypicolinoyl)glycinate (39). To a solution of **38** (10.5 g, 27.6 mmol) in DCM (200 mL) was added boron trifluoride etherate (30 mL). The mixture was stirred at 45 °C for 6 h under a nitrogen atmosphere. After cooling to room temperature, saturated NH_4Cl solution (200 mL) was added. The resulting mixture was stirred at room temperature for 2 h. The organic layer was separated, washed with water (300 mL \times 2) and saturated brine (300 mL \times 1), dried over anhydrous Na_2SO_4 , filtered and concentrated. The residue was recrystallized from DCM to afford the pale yellow solid **39** (5.86 g, 73.5%). mp 147.2–148.3 °C. ^1H NMR (300 MHz, CDCl_3): δ 3.67 (s, 3H), 4.07 (d, $J = 6.0$ Hz, 2H), 7.81 (d, $J = 1.8$ Hz, 1H), 8.30 (d, $J = 1.8$ Hz, 1H), 9.50 (t, $J = 6.0$ Hz, 1H), 12.39 (s, 1H). HRMS (ESI): calcd. for $\text{C}_9\text{H}_9\text{BrN}_2\text{O}_4$ $[\text{M} + \text{H}]^+$ 288.9819 and 290.9798, found 288.9816 and 290.9800.

4.2.5. Preparation of Methyl (3-hydroxy-5-((trimethylsilyl)ethynyl)picolinoyl)glycinate (41). A sealed 20 mL glass tube containing compound **39** (433 mg, 1.5 mmol), trimethylsilylacetylene (0.25 mL, 1.8 mmol), triethylamine (5 mL), $\text{Pd}(\text{PPh}_3)_2\text{Cl}_2$ (90 mg, 0.13 mmol), CuI (90 mg, 0.48 mmol) and acetonitrile (5 mL) was placed into the cavity of a microwave reactor and irradiated for 7 min, at 120 °C and power 300 W. After cooling to room temperature using an N_2 -flow, the tube was removed from the rotor. The reaction mixture was combined with dichloromethane (100 mL) and water (100 mL). The organic layer was separated, washed with saturated brine (50 mL \times 2) and then concentrated. The residue was purified by column chromatography (elute: petroleum ether) to afford the white solid **41** (413 mg, 90.0%). mp 90.1–92.5 °C. ^1H NMR (300

1
2
3 MHz, DMSO-*d*₆) δ 0.26 (s, 9H), 3.67 (s, 3H), 4.07 (d, *J* = 6.0 Hz, 2H), 7.52 (d, *J* = 1.5 Hz, 1H),
4
5 8.23 (d, *J* = 1.5 Hz, 1H), 9.53 (t, *J* = 6.0 Hz, 1H), 12.28 (s, 1H). EI-MS [M - H]⁻ = 305.1.
6
7

8 **4.2.6. Preparation of (5-Ethynyl-3-hydroxypicolinoyl)glycine (3).** To a solution of **41** (306 mg,
9 1 mmol) in methanol (15 mL) was added tetrabutylammonium fluoride trihydrate (379 mg, 1.2
10 mmol). The mixture was refluxed for 1 h. After cooling to room temperature, the mixture was
11 concentrated. The residue was dissolved in a mixture of THF (20 mL) and water (2 mL). Lithium
12 hydroxide (48 mg, 2 mmol) was added. The mixture was stirred at 35 °C for 1 h and then
13 concentrated. The resulting residue was dissolved in water (10 mL), and then acidified with 10%
14 HCl aqueous solution to pH = 3–4. The precipitate was collected, washed with water, and dried to
15 afford the white solid **3** (185 mg, 84.1%). mp 168.0–169.7 °C. ¹H NMR (300 MHz, DMSO-*d*₆) δ
16 3.98 (d, *J* = 6.0 Hz, 2H), 4.64 (s, 1H), 7.56 (d, *J* = 1.5 Hz, 1H), 8.25 (d, *J* = 1.5 Hz, 1H), 9.36 (s,
17 1H), 12.37 (s, 1H), 12.83 (brs, 1H). ¹³C NMR (75 MHz, DMSO-*d*₆) δ 79.52, 86.26, 123.73, 128.26,
18 130.62, 142.08, 156.40, 168.35, 170.28, 200.52. HRMS (ESI): calcd. for C₁₀H₈N₂O₄ [M + H]⁺
19 221.0557, found 211.0553. HPLC: t_R = 2.858 min, 99.4%.
20
21
22
23
24
25
26
27
28
29
30
31
32
33
34
35
36

37 **4.2.7. General Procedure for the Preparation of Compounds 4–34.** A sealed 20 mL glass tube
38 containing compound **39** (432 mg, 1.5 mmol), **42a–42ae** (3 mmol), *N,N*-diisopropylethylamine (5
39 mL), Pd(PPh₃)₂Cl₂ (60 mg, 0.86 mmol), CuI (60 mg, 0.32 mmol), and DMF (5 mL) was placed
40 into the cavity of a microwave reactor and irradiated for 15 min, at 120 °C and power 300 W. After
41 cooling to room temperature using an N₂-flow, the tube was removed from the rotor. The reaction
42 mixture was combined with dichloromethane (100 mL) and water (100 mL). The organic layer
43 was separated, washed with saturated brine (50 mL × 2) and then concentrated. The residue was
44 dissolved in a mixture of THF (20 mL) and water (10 mL). Lithium hydroxide (381 mg, 9.0 mmol)
45 was added to the solution. The mixture was stirred at 35 °C for 1 h and then the organic solvent
46
47
48
49
50
51
52
53
54
55
56
57
58
59
60

1
2
3 THF was evaporated. The resulting solution was acidified with 10% HCl to pH = 3–4 and then
4
5 extracted with DCM (20 mL × 4). The combined organic layer was washed with saturated brine
6
7 (20 mL) and then concentrated. The resulting residue was purified by column chromatography
8
9 (eluent: 20:1 DCM/MeOH) to afford compounds **4-34**.

10
11
12 4.2.7.1. (5-(3,3-Dimethylbut-1-yn-1-yl)-3-hydroxypicolinoyl)glycine (**4**). Pale yellow solid. Yield
13
14 71.6%. mp 168.0–169.7 °C. ¹H NMR (300 MHz, DMSO-*d*₆) δ 1.29 (s, 9H), 3.94 (d, *J* = 6.0 Hz,
15
16 2H), 7.38 (d, *J* = 1.5 Hz, 1H), 8.11 (d, *J* = 1.5 Hz, 1H), 9.37 (s, 1H), 12.34 (s, 1H). HRMS (ESI):
17
18 calcd. for C₁₄H₁₇N₂O₄ [M + H]⁺ 277.1183, found 277.189. HPLC: t_R = 8.563 min, 100.0%.
19
20
21

22 4.2.7.2. (5-(Cyclopropylethynyl)-3-hydroxypicolinoyl)glycine (**5**). Yield 59.4%. White solid. mp
23
24 182.0–184.5 °C. ¹H NMR (300 MHz, DMSO-*d*₆) δ 0.82–0.85 (m, 2H), 0.94–0.98 (m, 2H),
25
26 1.52–1.68 (m, 1H), 3.98 (d, *J* = 6.0 Hz, 2H), 7.42 (d, *J* = 1.5 Hz, 2H), 8.15 (d, *J* = 1.5 Hz, 1H),
27
28 9.42 (s, 1H), 12.36 (s, 1H). HRMS (ESI): calcd. for C₁₃H₁₂N₂O₄ [M + H]⁺ 261.0870, found
29
30 261.0887. HPLC: t_R = 5.673 min, 97.3%.
31
32
33

34 4.2.7.3. (3-Hydroxy-5-(phenylethynyl)picolinoyl)glycine (**6**). Yield 52.8%. Yellow solid. mp
35
36 198.8–200.7 °C. ¹H NMR (300 MHz, DMSO-*d*₆) δ 3.91 (d, *J* = 5.7 Hz, 2H), 7.47–7.49 (m, 3H),
37
38 7.61–7.64 (m, 3H), 8.35–8.36 (m, 1H), 9.44 (t, *J* = 6.0 Hz, 1H), 12.45 (s, 1H). HRMS (ESI): calcd.
39
40 for C₁₆H₁₂N₂O₄ [M + H]⁺ 297.0870, found 296.0878. HPLC: t_R = 8.23 min, 96.2%.
41
42
43

44 4.2.7.4. (5-([1,1'-Biphenyl]-4-ylethynyl)-3-hydroxypicolinoyl)glycine (**7**). Yield 58.9%. Brown
45
46 solid. mp 206.6–208.3 °C. ¹H NMR (300 MHz, DMSO-*d*₆) δ 3.98 (d, *J* = 6.0 Hz, 2H), 7.14–7.39
47
48 (m, 5H), 7.45–8.35 (m, 5H), 8.35 (s, 1H), 9.39 (t, *J* = 6.3 Hz, 1H), 12.41 (s, 1H). HRMS (ESI):
49
50 calcd. for C₂₂H₁₆N₂O₄ [M + H]⁺ 373.1183, found 373.1190. HPLC: t_R = 14.852 min, 100.0%.
51
52
53
54
55
56
57
58
59
60

1
2
3 4.2.7.5. (3-Hydroxy-5-(3-phenoxyprop-1-yn-1-yl)picolinoyl)glycine (**8**). Yield 68.6%. White
4 solid. mp 217.6–219.2 °C. ¹H NMR (300 MHz, DMSO-*d*₆) δ 3.92 (d, *J* = 6.0 Hz, 2H), 5.10 (s, 2H),
5 6.97–7.37 (m, 5H), 7.52 (d, *J* = 1.5 Hz, 1H), 8.21 (d, *J* = 1.5 Hz, 1H), 9.31 (s, 1H). HRMS (ESI):
6 7.52 (d, *J* = 1.5 Hz, 1H), 8.21 (d, *J* = 1.5 Hz, 1H), 9.31 (s, 1H). HRMS (ESI):
8 calcd. for C₁₇H₁₄N₂O₅ [M + H]⁺ 327.0976, found 327.0976. HPLC: t_R = 6.981 min, 97.2%.
9

10
11
12 4.2.7.6. (3-Hydroxy-5-(3-(phenylamino)prop-1-yn-1-yl)picolinoyl)glycine (**9**). Yield 30.1%.
13 Brown solid. mp 94.3–97.6 °C. ¹H NMR (300 MHz, DMSO-*d*₆) δ 3.86 (d, *J* = 5.1 Hz, 2H), 4.08
14 (s, 2H), 6.01 (s, 1H), 6.50–6.61 (m, 3H), 7.01–7.04 (m, 2H), 7.31 (d, *J* = 1.5 Hz, 1H), 8.03 (d, *J* =
15 1.5 Hz, 1H), 9.23 (t, *J* = 5.7 Hz, 1H), 12.30 (brs, 1H). HRMS (ESI): calcd. for C₁₇H₁₅N₃O₄ [M +
16 H]⁺ 326.1136, found 326.1138. HPLC: t_R = 6.202 min, 97.0%.
17
18
19

20 4.2.7.7. (3-Hydroxy-5-(3-(methyl(phenyl)amino)prop-1-yn-1-yl)picolinoyl)glycine (**10**). Yield
21 37.0%. Yellow solid. mp 162.3–163.7 °C. ¹H NMR (300 MHz, DMSO-*d*₆) δ 2.95 (s, 3H), 3.57 (s,
22 2H), 4.42 (s, 2H), 6.73–6.76 (m, 1H), 6.89–6.92 (m, 2H), 7.20–7.22 (m, 2H), 7.31 (s, 1H), 8.05
23 (s, 1H), 8.89 (s, 1H). HRMS (ESI): calcd. for C₁₈H₁₇N₃O₄ [M + H]⁺ 340.1292, found 340.1290.
24 HPLC: t_R = 8.743 min, 97.2%.
25
26

27 4.2.7.8. (5-(3-(Diphenylamino)prop-1-yn-1-yl)-3-hydroxypicolinoyl)glycine (**11**). Yield 34.7%.
28 Brown solid. mp 99.4–101.1 °C. ¹H NMR (300 MHz, DMSO-*d*₆) δ 3.90 (d, *J* = 6.0 Hz, 2H), 4.76
29 (s, 2H), 6.78–6.97 (m, 7H), 7.22–7.36 (m, 5H), 8.05 (d, *J* = 1.5 Hz, 1H), 9.25 (s, 1H). HRMS
30 (ESI): calcd. for C₂₃H₁₉N₃O₄ [M + H]⁺ 402.1449, found 402.1441. HPLC: t_R = 17.077 min, 95.8%.
31
32
33

34 4.2.7.9. (5-(3-(2-Fluorophenoxy)prop-1-yn-1-yl)-3-hydroxypicolinoyl)glycine (**12**). Yield 34.9%.
35 White solid. mp 155.1–158.3 °C. ¹H NMR (300 MHz, DMSO-*d*₆) δ 3.93 (s, 2H), 5.18 (s, 2H),
36 6.99–7.01 (m, 1H), 7.21–7.35 (m, 3H), 7.51–7.63 (m, 1H), 8.20 (s, 1H), 9.32 (s, 1H), 12.48 (brs,
37 1H). HRMS (ESI): calcd. for C₁₇H₁₃FN₂O₅ [M + H]⁺ 345.0882, found 345.0879. HPLC: t_R = 7.196
38 min, 98.6%.
39
40
41
42
43
44
45
46
47
48
49
50
51
52
53
54
55
56
57
58
59
60

1
2
3 4.2.7.10. (5-(3-(3-Fluorophenoxy)prop-1-yn-1-yl)-3-hydroxypicolinoyl)glycine (**13**). Yield
4 37.7%. Yellow solid. mp 127.0–128.8 °C. ¹H NMR (300 MHz, DMSO-*d*₆) δ 3.97 (d, *J* = 6.0 Hz,
5 2H), 5.13 (s, 2H), 6.79–6.97 (m, 3H), 7.32–7.39 (m, 1H), 7.54 (d, *J* = 1.5 Hz, 1H), 8.22 (s, 1H),
6 9.41 (t, *J* = 6.0 Hz 1H), 12.41 (s, 1H), 12.85 (brs, 1H). HRMS (ESI): calcd. for C₁₇H₁₃FN₂O₅ [M
7 + H]⁺ 345.0882, found 345.0883. HPLC: t_R = 6.639 min, 98.7%.

8
9
10
11
12 4.2.7.11. (5-(3-(4-Fluorophenoxy)prop-1-yn-1-yl)-3-hydroxypicolinoyl)glycine (**14**). Yield
13 71.6%. Yellow solid. mp 173.6–175.3 °C. ¹H NMR (300 MHz, DMSO-*d*₆) δ 3.99 (d, *J* = 6.0 Hz,
14 2H), 5.16 (s, 2H), 7.12–7.26 (m, 4H), 7.59 (d, *J* = 1.5 Hz, 1H), 8.28 (d, *J* = 1.5 Hz, 1H), 9.38 (s,
15 1H), 12.40 (s, 1H). HRMS (ESI): calcd. for C₁₇H₁₃FN₂O₅ [M + H]⁺ 345.0882, found 345.0877.
16
17 HPLC: t_R = 7.670 min, 99.2%.

18
19
20 4.2.7.12. (5-(3-(2-Chlorophenoxy)prop-1-yn-1-yl)-3-hydroxypicolinoyl)glycine (**15**). Yield
21 41.0%. Brown solid. mp 154.6–156.2 °C. ¹H NMR (300 MHz, DMSO-*d*₆) δ 3.94 (d, *J* = 4.8 Hz,
22 2H), 5.22 (s, 2H), 7.01–7.07 (m, 1H), 7.33–7.57 (m, 4H), 8.21 (s, 1H), 9.34 (s, 1H), 12.37 (brs,
23 1H). HRMS (ESI): calcd. for C₁₇H₁₃N₂O₅ [M + H]⁺ 361.0586, found 361.0589. HPLC: t_R = 8.668
24 min, 95.9%.

25
26
27 4.2.7.13. (5-(3-(3-Chlorophenoxy)prop-1-yn-1-yl)-3-hydroxypicolinoyl)glycine (**16**). Yield
28 37.2%. White solid. mp 138.2–141.5 °C. ¹H NMR (300 MHz, DMSO-*d*₆) δ 3.97 (s, 2H), 5.22 (s,
29 2H), 7.01–7.46 (m, 4H), 7.54 (s, 1H), 8.37 (s, 1H), 9.53 (s, 1H), 12.40 (s, 1H), 12.85 (brs, 1H).
30
31 HRMS (ESI): calcd. for C₁₇H₁₃ClN₂O₅ [M + H]⁺ 361.0586, found 361.0583. HPLC: t_R = 7.093
32 min, 100.0%.

33
34
35 4.2.7.14. (5-(3-(4-Chlorophenoxy)prop-1-yn-1-yl)-3-hydroxypicolinoyl)glycine (**17**). Yield
36 82.3%. White solid. mp 131.5–133.2 °C. ¹H NMR (300 MHz, DMSO-*d*₆) δ 3.96 (d, *J* = 5.1 Hz,
37 2H), 5.10 (s, 2H), 7.06–7.08 (m, 2H), 7.36–7.38 (m, 2H), 7.52 (s, 1H), 8.20 (s, 1H), 9.38 (s, 1H),
38
39

1
2
3 12.39 (brs, 1H). ^{13}C NMR (75 MHz, $\text{DMSO-}d_6$) δ 41.09, 56.30, 82.66, 89.88, 116.69, 123.36,
4
5 125.13, 127.95, 129.29, 130.75, 141.71, 156.03, 156.45, 168.06, 170.22. HRMS (ESI): calcd. for
6
7 $\text{C}_{17}\text{H}_{13}\text{ClN}_2\text{O}_5$ $[\text{M} + \text{H}]^+$ 361.0586, found 361.0583. HPLC: $t_{\text{R}} = 8.37$ min, 99.3%.

8
9
10 4.2.7.15. (3-Hydroxy-5-(3-(2-methylphenoxy)prop-1-yn-1-yl)picolinoyl)glycine (**18**). Yield
11
12 36.6%. Brown solid. mp 165.1–168.4 °C. ^1H NMR (300 MHz, $\text{DMSO-}d_6$) δ 2.17 (s, 3H), 3.83 (d,
13
14 $J = 5.1$ Hz, 2H), 5.10 (s, 2H), 6.89 (t, $J = 7.2$ Hz, 1H), 7.07–7.21 (m, 3H), 7.49 (s, 1H), 8.19 (s,
15
16 1H), 9.18 (s, 1H). HRMS (ESI): calcd. for $\text{C}_{18}\text{H}_{16}\text{N}_2\text{O}_5$ $[\text{M} + \text{H}]^+$ 341.1132, found 341.1126. HPLC:
17
18 $t_{\text{R}} = 11.246$ min, 98.9%.

19
20
21 4.2.7.16. (3-Hydroxy-5-(3-(3-methylphenoxy)prop-1-yn-1-yl)picolinoyl)glycine (**19**). Yield
22
23 48.7%. Yellow solid. mp 136.8–138.5 °C. ^1H NMR (300 MHz, $\text{DMSO-}d_6$) δ 2.28 (s, 3H), 3.95 (d,
24
25 $J = 5.7$ Hz, 2H), 5.06 (s, 2H), 6.79–6.85 (m, 3H), 7.19 (t, $J = 7.5$ Hz, 1H), 7.51 (s, 1H), 8.20 (s,
26
27 1H), 9.33 (s, 1H), 12.48 (brs, 1H). HRMS (ESI): calcd. for $\text{C}_{18}\text{H}_{16}\text{N}_2\text{O}_5$ $[\text{M} + \text{H}]^+$ 341.1132, found
28
29 341.1126. HPLC: $t_{\text{R}} = 10.501$ min, 99.5%.

30
31
32 4.2.7.17. (3-Hydroxy-5-(3-(4-methylphenoxy)prop-1-yn-1-yl)picolinoyl)glycine (**20**). Yield
33
34 43.2%. Pale yellow solid. mp 240.8–242.5 °C. ^1H NMR (300 MHz, $\text{DMSO-}d_6$) δ 2.21 (s, 3H), 3.80
35
36 (d, $J = 4.8$ Hz, 2H), 5.02 (s, 2H), 6.92 (d, $J = 8.4$ Hz, 2H), 7.11 (d, $J = 8.4$ Hz, 2H), 7.47 (s, 1H),
37
38 8.17 (s, 1H), 9.14 (s, 1H). ^{13}C NMR (75 MHz, $\text{DMSO-}d_6$) δ 20.05, 42.76, 55.99, 82.48, 90.10,
39
40 114.74, 123.14, 128.04, 129.84, 130.09, 131.27, 141.01, 155.14, 156.99, 167.02, 169.38. HRMS
41
42 (ESI): calcd. for $\text{C}_{18}\text{H}_{16}\text{N}_2\text{O}_5$ $[\text{M} + \text{H}]^+$ 341.1132, found 341.1135. HPLC: $t_{\text{R}} = 11.861$ min, 98.4%.

43
44
45 4.2.7.18. (3-Hydroxy-5-(3-(2-(trifluoromethyl)phenoxy)prop-1-yn-1-yl)picolinoyl)glycine (**21**).
46
47 Yield 62.2%. Yellow solid. mp 182.9–184.6 °C. ^1H NMR (300 MHz, $\text{DMSO-}d_6$) δ 2.07 (s, 2H),
48
49 3.86 (d, $J = 6.3$ Hz, 2H), 5.29 (s, 2H), 7.16 (t, $J = 7.5$ Hz, 1H), 7.44 (d, $J = 8.4$ Hz, 1H), 7.50 (d, J
50
51
52
53
54
55
56
57
58
59
60

1
2
3 = 2.1 Hz, 1H), 7.64–7.69 (m, 2H), 8.19 (d, $J = 1.8$ Hz, 1H), 9.25 (s, 1H). HRMS (ESI): calcd. for
4 $C_{18}H_{13}F_3N_2O_5$ $[M + H]^+$ 395.0850, found 395.0841. HPLC: $t_R = 7.763$ min, 98.1%.
5
6

7
8 4.2.7.19. (3-Hydroxy-5-(3-(3-(trifluoromethyl)phenoxy)prop-1-yn-1-yl)picolinoyl)glycine (**22**).
9
10 Yield 67.7%. Brown solid. mp 94.3–96.1 °C. 1H NMR (300 MHz, DMSO- d_6) δ 3.99 (d, $J = 6.0$
11 Hz, 2H), 5.25 (s, 2H), 7.36–7.43 (m, 3H), 7.54–7.62 (m, 2H), 8.22 (d, $J = 1.5$ Hz, 1H), 9.43 (t, J
12 = 6.0 Hz, 1H), 12.44 (s, 1H). HRMS (ESI): calcd. for $C_{18}H_{13}F_3N_2O_5$ $[M + H]^+$ 395.0850, found
13 395.0842. HPLC: $t_R = 9.819$ min, 97.9%.
14
15
16
17
18

19
20 4.2.7.20. (3-Hydroxy-5-(3-(4-(trifluoromethyl)phenoxy)prop-1-yn-1-yl)picolinoyl)glycine (**23**).
21
22 Yield 53.0%. Pale yellow solid. mp 142.3–145.0 °C. 1H NMR (300 MHz, DMSO- d_6) δ 3.95 (d, J
23 = 6.0 Hz, 2H), 5.24 (s, 2H), 7.26 (d, $J = 8.7$ Hz, 2H), 7.57 (d, $J = 1.8$ Hz, 1H), 7.74 (d, $J = 8.7$ Hz,
24 2H), 8.24 (d, $J = 1.8$ Hz, 1H), 9.37 (t, $J = 6.0$ Hz, 1H), 12.47 (brs, 1H). HRMS (ESI): calcd. for
25 $C_{18}H_{13}F_3N_2O_5$ $[M + H]^+$ 395.0850, found 395.0846. HPLC: $t_R = 9.109$ min, 96.4%.
26
27
28
29
30

31
32 4.2.7.21. (3-Hydroxy-5-(3-(2-methoxyphenoxy)prop-1-yn-1-yl)picolinoyl)glycine (**24**). Yield
33 43.3%. Yellow solid. mp 138.7–140.4 °C. 1H NMR (300 MHz, DMSO- d_6) δ 3.77 (s, 3H), 3.97 (d,
34 $J = 6.0$ Hz, 2H), 5.06 (s, 2H), 6.97–7.00 (m, 3H), 7.11 (d, $J = 1.8$ Hz, 1H), 7.52 (d, $J = 1.8$ Hz,
35 1H), 8.21 (d, $J = 1.8$ Hz, 1H), 9.40 (s, 1H), 12.40 (s, 1H). HRMS (ESI): calcd. for $C_{18}H_{16}N_2O_6$ $[M$
36 + $H]^+$ 357.1082, found 357.1078. HPLC: $t_R = 5.095$ min, 96.3%.
37
38
39
40
41
42
43

44 4.2.7.22. (3-Hydroxy-5-(3-(3-methoxyphenoxy)prop-1-yn-1-yl)picolinoyl)glycine (**25**). Yield
45 48.7%. Brown solid. mp 111.0–112.6 °C. 1H NMR (300 MHz, DMSO- d_6) δ 3.73 (s, 3H), 3.96 (d,
46 $J = 6.0$ Hz, 2H), 5.27 (s, 2H), 6.59–6.64 (m, 3H), 7.17–7.23 (m, 1H), 7.52 (d, $J = 1.8$ Hz, 1H),
47 8.22 (d, $J = 1.8$ Hz, 1H), 9.40 (s, 1H). HRMS (ESI): calcd. for $C_{18}H_{16}N_2O_6$ $[M + H]^+$ 357.1082,
48 found 357.1079. HPLC: $t_R = 6.363$ min, 95.3%.
49
50
51
52
53
54
55
56
57
58
59
60

1
2
3 4.2.7.23. (3-Hydroxy-5-(3-(4-methoxyphenoxy)prop-1-yn-1-yl)picolinoyl)glycine (**26**). Yield
4 63.2%. Pale yellow solid. mp 166.7–168.4 °C. ¹H NMR (300 MHz, DMSO-*d*₆) δ 3.70 (s, 3H), 3.95
5 (d, *J* = 6.0 Hz, 2H), 5.02 (s, 2H), 6.89 (d, *J* = 9.0 Hz, 2H), 7.00 (d, *J* = 9.0 Hz, 2H), 7.52 (s, 1H),
6 8.21 (s, 1H), 9.37 (s, 1H). HRMS (ESI): calcd. for C₁₈H₁₆N₂O₆ [M + H]⁺ 357.1082, found 357.1073.
7
8 HPLC: t_R = 7.447 min, 99.0%.
9

10
11 4.2.7.24. (5-(3-(4-Ethylphenoxy)prop-1-yn-1-yl)-3-hydroxypicolinoyl)glycine (**27**). Yield 52.8%.
12 White solid. mp 228.8–230.5 °C. ¹H NMR (300 MHz, DMSO-*d*₆) δ 1.14 (t, *J* = 7.5 Hz, 3H),
13 2.49–2.55 (m, 2H), 3.65 (d, *J* = 4.8 Hz, 2H), 5.04 (s, 2H), 6.94 (d, *J* = 8.7 Hz, 2H), 7.15 (d, *J* = 8.7
14 Hz, 2H), 7.46 (d, *J* = 1.2 Hz, 1H), 8.16 (d, *J* = 1.2 Hz, 1H), 9.00 (s, 1H). HRMS (ESI): calcd. for
15 C₁₉H₁₈N₂O₅ [M + H]⁺ 355.1289, found 355.1289. HPLC: t_R = 13.190 min, 98.1%.
16
17

18 4.2.7.25. (5-(3-(4-Cyanophenoxy)prop-1-yn-1-yl)-3-hydroxypicolinoyl)glycine (**28**). Yield 34.9%.
19 Brown solid. mp 152.8–153.3 °C. ¹H NMR (300 MHz, DMSO-*d*₆) δ 3.85 (d, *J* = 5.7 Hz, 2H), 5.14
20 (s, 1H), 7.13 (d, *J* = 8.7 Hz, 2H), 7.44 (s, 1H), 7.73 (d, *J* = 8.7 Hz, 2H), 8.21 (s, 1H), 9.25 (s, 1H).
21 HRMS (ESI): calcd. for C₁₈H₁₃N₃O₅ [M + H]⁺ 352.0928, found 352.0930. HPLC: t_R = 4.456 min,
22 96.2%.
23
24

25 4.2.7.26. (5-(3-([1,1'-Biphenyl]-4-yloxy)prop-1-yn-1-yl)-3-hydroxypicolinoyl)glycine (**29**). Yield
26 44.4%. Brown solid. mp 82.8–84.4 °C. ¹H NMR (300 MHz, DMSO-*d*₆) δ 3.97 (d, *J* = 6.0 Hz, 2H),
27 5.15 (s, 2H), 7.13 (d, *J* = 9.0 Hz, 2H), 7.28–7.33 (m, 1H), 7.43–7.45 (m, 2H), 7.55–7.58 (m, 1H),
28 7.61–7.65 (m, 4H), 8.23 (d, *J* = 1.8 Hz, 1H), 9.42 (t, *J* = 6.0 Hz, 1H), 12.41 (s, 1H). HRMS (ESI):
29 calcd. for C₂₃H₁₈N₂O₅ [M + H]⁺ 403.1289, found 403.1288. HPLC: t_R = 15.542 min, 95.6%.
30
31

32 4.2.7.27. (3-Hydroxy-5-(3-(naphthalen-1-yloxy)prop-1-yn-1-yl)picolinoyl)glycine (**30**). Yield
33 68.9%. Brown solid. mp 102.7–104.5 °C. ¹H NMR (300 MHz, DMSO-*d*₆) δ 3.96 (d, *J* = 6.0 Hz,
34 2H), 5.32 (s, 2H), 7.14–7.16 (d, *J* = 7.5 Hz, 1H), 7.35–7.63 (m, 5H), 7.87–7.90 (m, 1H), 8.16–8.19
35
36
37
38
39
40
41
42
43
44
45
46
47
48
49
50
51
52
53
54
55
56
57
58
59
60

(m, 1H), 8.23 (s, 1H), 9.39 (t, $J = 6.0$ Hz, 1H), 12.40 (s, 1H), 12.48 (brs, 1H). HRMS (ESI): calcd. for $C_{21}H_{16}N_2O_5$ $[M + H]^+$ 377.1132, found 377.1126. HPLC: $t_R = 11.531$ min, 96.7%.

4.2.7.28. (5-(3-(2,4-Dichlorophenoxy)prop-1-yn-1-yl)-3-hydroxypicolinoyl)glycine (**31**). Yield 37.8%. Brown solid. mp 125.2–126.9 °C. 1H NMR (300 MHz, DMSO- d_6) δ 3.91 (d, $J = 6.0$ Hz, 2H), 5.24 (s, 2H), 7.34 (d, $J = 9.0$ Hz, 2H), 7.42–7.46 (m, 1H), 7.54 (d, $J = 1.8$ Hz, 1H), 7.62 (d, $J = 2.4$ Hz, 1H), 8.21 (d, $J = 1.8$ Hz, 1H), 9.34 (s, 1H). HRMS (ESI): calcd. for $C_{17}H_{12}Cl_2N_2O_5$ $[M + H]^+$ 395.0197, found 395.0188. HPLC: $t_R = 11.521$ min, 96.0%.

4.2.7.29. (5-(3-(3,4-Dichlorophenoxy)prop-1-yn-1-yl)-3-hydroxypicolinoyl)glycine (**32**). Yield 39.0%. Brown solid. mp 137.7–139.4 °C. 1H NMR (300 MHz, DMSO- d_6) δ 3.98 (d, $J = 6.0$ Hz, 2H), 5.19 (s, 2H), 7.11 (dd, $J_1 = 3.0$ Hz, $J_2 = 9.0$ Hz, 1H), 7.39 (d, $J = 3.0$ Hz, 1H), 7.58 (d, $J = 1.8$ Hz, 1H), 7.61 (d, $J = 9.0$ Hz, 1H), 8.24 (d, $J = 1.8$ Hz, 1H), 9.42 (t, $J = 6.0$ Hz, 1H), 11.45 (brs, 1H). HRMS (ESI): calcd. for $C_{17}H_{12}Cl_2N_2O_5$ $[M + H]^+$ 395.0197, found 395.0188. HPLC: $t_R = 12.009$ min, 97.4%.

4.2.7.30. (5-(((4-Chlorobenzyl)oxy)ethynyl)-3-hydroxypicolinoyl)glycine (**33**). Yield 31.0%. White solid. mp 112.8–114.4 °C. 1H NMR (300 MHz, DMSO- d_6) δ 3.99 (d, $J = 6.3$ Hz, 2H), 4.52 (s, 2H), 4.63 (s, 2H), 7.40–7.46 (m, 4H), 7.57 (d, $J = 1.8$ Hz, 1H), 8.26 (d, $J = 1.8$ Hz, 1H), 9.42 (t, $J = 6.0$ Hz, 1H), 12.42 (s, 1H), 12.93 (brs, 1H). ^{13}C NMR (75 MHz, DMSO- d_6) δ 40.73, 57.55, 70.37, 82.06, 91.40, 123.90, 127.89, 128.27, 129.67, 130.46, 132.24, 136.65, 141.81, 156.45, 168.34, 170.26. HRMS (ESI): calcd. for $C_{18}H_{15}ClN_2O_5$ $[M + H]^+$ 375.0743, found 375.0740. HPLC: $t_R = 8.658$ min, 99.2%.

4.2.7.31. (5-(((4-Chlorophenoxy)ethynyl)-3-hydroxypicolinoyl)glycine (**34**). Yield 36.0%. Brown solid. mp 128.2–129.9 °C. 1H NMR (300 MHz, DMSO- d_6) δ 2.85 (d, $J = 6.3$ Hz, 2H), 3.57 (t, $J = 6.9$ Hz, 2H), 3.97 (d, $J = 5.4$ Hz, 2H), 4.43 (s, 2H), 7.21–7.34 (m, 3H), 7.55–7.64 (m, 2H),

1
2
3 8.21 (s, 1H), 9.37 (s, 1H), 12.39 (s, 1H). ¹³C NMR (75 MHz, DMSO-*d*₆) δ 40.36, 57.55, 62.35,
4
5 70.34, 81.99, 91.12, 123.55, 127.96, 128.27, 129.78, 130.63, 132.39, 137.03, 141.60, 156.44,
6
7 167.86, 170.14. HRMS (ESI): calcd. for C₁₉H₁₇ClN₂O₅ [M + H]⁺ 389.0899, found 389.0892.
8
9
10 HPLC: t_R = 9.687 min, 95.8%.

11
12 **4.3. Molecular Modeling.** The complex structure of PHD2 and its inhibitor (PDB: 2G19) was
13
14 obtained from the PDB website.¹⁷ The structure files of protein and compounds for docking were
15
16 both prepared using Discovery Studio (DS) 4.0. The water molecule HOH601, being conserved in
17
18 the binding sites of PHD2, was kept for docking. Residues of PHD2 around the native ligand
19
20 (radius = 10 Å) were defined as the binding sites for docking. Compounds were docked into the
21
22 binding sites using the software GOLD 5.1. Docking procedures were performed using the default
23
24 setting with 100 genetic algorithm (GA) runs of ligands. For each GA run, a maximum of 125,000
25
26 operations were performed. When the top ten solutions possessed RMSD values within 1.5 Å,
27
28 docking was terminated.
29
30
31

32
33 **4.4 In Vitro Assay for PHD2.** *In Vitro PHD2 Fluorescence Polarization Assay.* The experimental
34
35 buffer contained 10 μM MnCl₂, 10 mM Hepes, 150 mM NaCl, 0.05% Tween-20 and 20 μM of 2-
36
37 OG at pH 7.4. FITC-HIF-1α (556–574, DLDLEMLAPYIPMDDDFQL) peptides were used as
38
39 probes, and the reactions performed in 384 black well plates (#3575, Corning) with a total reaction
40
41 volume of 60 μL (20 μL PHD2 protein, 20 μL FITC-based probe, and 20 μL tested compounds).
42
43 PHD2 (181-426), which is reported to have similarly bioactivity to the full-length PHD2 (Nanjing
44
45 Zoombio Biotechnology), and the FP assay (λ_{ex}=485 ± 25 nm; λ_{em}=535 ± 25 nm) were recorded
46
47 by SpectraMax GeminiXS (Molecular Devices, Sunnyvale, CA.). The data were analyzed using
48
49 GraphPad Prism 7.0.
50
51
52
53
54
55
56
57
58
59
60

1
2
3 *AlphaScreen Assay.* To verify whether the compound **17** has good PHD2 selectivity, Alphascreen
4 assay was used to evaluate the compound's activity on other 2-OG-dependent dioxygenases
5 (JMJD1A, JMJD2A, and JMJD3). The Alphascreen IgG kit provides the necessary reagents for
6 the test. The test was performed in a 384-well white plate (Perkin Elmer). The buffer solution
7 contained 50 mM HEPES, BSA (0.1% w / v), Tween-20 (0.01% v / v), 3 μ L of the test compound
8 and 4 μ L of dioxygenase mixed at room temperature for 30 minutes. 3 μ L of peptide substrate was
9 added; 5 μ L of anti-mouse receptor beads and 5 μ L of the substrate antibodies were then added to
10 the reaction system after the enzymatic reaction and incubated for 30 minutes at room temperature,
11 10 μ L of AphaScreen Streptavidin-coupled donor beads were added. The 384-well white plate was
12 investigated in an AlphaScreen microplate reader (PerkinElmer).
13
14
15
16
17
18
19
20
21
22
23
24
25

26 *Western-blot.* Hep3B cells were treated with **17** and **FG-4592** at the corresponding concentrations
27 for 10 h. The protein concentration of the nuclear extracts was further investigated by BCA assay.
28 Equal amounts of nuclear protein extracts were separated by SDS-PAGE and then investigated
29 using a western blot. The membrane was then incubated with specific antibodies including anti-
30 HIF-1 α , anti-HIF-2 α , and anti-LaminB (Bioworld, USA). LaminB was used as the internal
31 control. Lastly, images were visualized using the Odyssey Infrared Imaging System (LI-COR,
32 Lincoln, Nebraska, USA).
33
34
35
36
37
38
39
40
41

42 *HIF-Luciferase Reporter Assay.* Extraction of HIF-1 α and SV40 plasmids were conducted using
43 the TIANGEN BIOTECH kit. MCF-7 cells in the logarithmic phase were added to 48-well plates
44 and cultured for 24 h. Cells in each well culture plate were transfected with 0.4 μ g plasmids using
45 1 μ L Lipofectamine 2000 Transfection Reagent (Invitrogen, Calif., USA) for about 6 h. After
46 incubation for 24 h with **17**, the cells were lysed by the addition of lysate; renilla fluorescein
47 substrate and firefly fluorescein substrate were then both added to detect the chemiluminescence
48
49
50
51
52
53
54
55
56
57
58
59
60

1
2
3 signals on Thermo LUMINOSKAN ASCENT (Thermo Scientific, USA). The data were analyzed
4
5 by GraphPad Prism 7.0.
6

7
8 *EPO gene analysis.* The RNA extraction and gene expression of EPO was determined by qRT-
9
10 PCR. The total RNA of **17**-treated Hep3B cells was isolated using TRIzol (Invitrogen); qRT-PCR
11
12 analyses of EPO (5'-GGAGGCCGAGAATATCACGAC-3' (sense primer), 5'-
13
14 CCCTGCCAGACTTCTACGG-3' (antisense primer)) was performed by using the STEPONE
15
16 SYSTEM Fast Real Time PCR system (Applied Biosystems). Human GADPH 5'-
17
18 AGGTGAAGGTCGGAGTCAAC-3' (sense) and 5'-CGCTCCTGGAAGATGGTGAT-3'.
19
20 (antisense) were used for normalization. The qRT-PCR analysis of EPO was set out on the 7500
21
22 Fast Real Time PCR system (Applied Biosystems). Each cycle of PCR included a 5 s at 95 °C
23
24 denaturation and a 30 s at 60 °C annealing and extension stage. A total of 40 cycles were
25
26 determined.
27
28
29

30
31 *Cell-based EPO Elisa Assay.* Hep3B cells in the logarithmic growth phase were seeded into a 96-
32
33 well plate and treated with the compound **17** and **FG-4592** for 24 h. Subsequently, the cells were
34
35 collected for testing using the Human Erythropoietin Quantikine IVD ELISA Kit (ab119522).
36
37 After processing the samples, 50 µL stop solution was added to each well. The absorbance (OD
38
39 value) of each well was sequentially measured at 450 nM wavelength (the measurement should be
40
41 performed immediately after adding the stop solution).
42
43
44

45 **4.5 Pharmacodynamic assay. In Vivo Plasma EPO Increased Assay.** Plasma EPO was evaluated
46
47 using the Erythropoietin Quantikine ELISA Kit for Mice/Rats (MEP00B). Representative
48
49 compounds were formulated in 10 mM NaOH (aq). C57BL/6 (n=5) mice were dosed *iv* and *po* at
50
51 0.2 mL (15 mg/kg). After 4 hours, the test sample of blood was obtained via orbital venous plexus.
52
53 Subsequently, the plasmas were stored at -80 °C, and were quickly detected by EPO ELISA.
54
55
56
57
58
59
60

1
2
3 Results were compared to the vehicle controls and the assay was quality-controlled with the
4
5 positive compound **FG-4592**.

6
7 *In Vivo Reticulocytes Increased Assay.* **17** and **FG-4592** were formulated in 10 mM NaOH (aq)
8
9 solution. Mice (C57BL/6, n=5 per dose level) were dosed *po* at a volume of 0.2 ml. On days 3 and
10
11 4 post-dose (5, 10, 25, and 50 mg/kg), the test sample was obtained via the orbital venous plexus.
12
13 Subsequently, the plasmas were stored at -80 °C and were analyzed for reticulocytes in Zhongda
14
15 hospital (Nanjing, China).
16
17
18
19

20
21 *Improvement in Anemia Induced by Cisplatin Administration.* C57BL/6 mice (male) were treated
22
23 with cisplatin (*po*, 7mg/kg) on days 0, 7, 14, and 28 of the experiment.³⁴ On the 29th day, the
24
25 animals were randomized into vehicle and treated-groups (n=6); then, compound **17** and **FG-4592**
26
27 (10 and 25 mg/kg) were administrated for the treatment of anemia caused by cisplatin. The mice
28
29 were treated with the compounds every alternate day for a month. The test sample was obtained
30
31 via the orbital venous plexus. Subsequently, routine blood examinations were performed and
32
33 analyzed immediately by the Jiangsu Hospital Integrated Traditional and Western Medicine
34
35 (Nanjing, China).
36
37
38
39

40 **4.5 Pharmacokinetic assay. Microsomal and hepatocyte Stability.** **17** was preincubated with
41
42 different species' microsomes (0.5 mg/mL) at 1 μM for 5 min at 37°C in 100 mM PBS buffer (PH
43
44 7.4). Subsequently, the bioreaction was catalyzed by adding NADPH (1 mM). After co-incubation
45
46 for varying times (0, 15, 30, 60, 90 and 120 min) at 37°C, the bioreaction was terminated by cold
47
48 acetonitrile. The clear supernatant samples were investigated by LC-MS/MS. Compound **17** (100
49
50 μM) was incubated with rat/mice hepatocyte and human L-02 cells for varying times (0, 15, 30,
51
52 60, 90 and 120 min). The samples were centrifuged at 4000 rpm for 20 min and the supernatants
53
54 analyzed by LC-MS/MS.
55
56
57
58
59
60

1
2
3 *CYP450 Inhibition.* The CYP450 inhibition activity of **17** on four major isozymes (CYP1A2,
4 CYP2C1, CYP2C9, CYP2D6, and CYP3A4) was evaluated by LC-MS/MS. Equal volumes (25
5 μL) of diluted microsomes (0.2 mg/mL final), **17**, the positive control compounds, and specific
6 CYP450 isozymes (10 μM , CYP1A2, CYP2C1, CYP2C9, CYP2D6, testosterone and midazolam
7 for CYP3A4, respectively) were preincubated for 5 min at 37 °C. Subsequently, the bioreaction
8 was catalyzed by adding NADPH (1 mM). After 20 min, the reaction was terminated by adding
9 cold acetonitrile. The clear supernatant samples were investigated using the LC-MS/MS method.
10
11
12
13
14
15
16
17
18
19

20 *In Vivo Pharmacokinetic Assay.* The animals (six healthy male beagle dogs, weight 11 ± 1 kg,
21 three for *po* and three for *iv*; eight SD rats, weight 260 ± 20 g, four for *po* and four for *iv*) were
22 administered with **17**. For *po* administration, the test compound (2 mg/kg, at 1 mg/mL) was
23 administered orally to both animals; for *iv* administration, the test compound (0.5 mg/kg for dogs,
24 1.0 mg/kg for rats, at 1 mg/mL) was administered intravenously to the animals. Blood samples
25 were collected at times 0, 1 min, 5 min, 15 min, 30 min, 1 h, 2 h, 4 h, 6 h, 8 h for the *iv* group, and
26 at 0, 5 min, 15 min, 30 min, 1 h, 2 h, 4 h, 6 h, 8 h after administration for the *po* group. The resulting
27 plasma samples were stored at -80 °C and analyzed by LC-MS/MS assay.
28
29
30
31
32
33
34
35
36
37
38

39 **4.6 Safety assay. MTT assay.** The typical cells were seeded in 96-well plates. Compound **17** was
40 added to the wells at concentrations of 10 to 100 μM , then incubated at 37 °C in a 5% CO_2
41 atmosphere for 72 h. MTT solution (5 mg/mL) was added and incubated with the cells for 4 h. The
42 solutions were removed and the formazan was dissolved in 150 μL of DMSO buffer. The
43 absorbance of the samples was detected at 570 nm.
44
45
46
47
48
49
50
51
52
53
54
55
56
57
58
59
60

1
2
3 *hERG assay.* The whole-cell patch clamp technique was used in this assay. Transfected HEK 293
4 cells and transfected CHO cells were used which can express the hERG potassium channel stably;
5
6 hERG toxicity of **17** was conducted according to the reported method.³¹
7
8
9

10 *Subacute toxicity.* SD rats were divided into 16 groups (n = 6), including 15 mg/kg, 50 mg/kg, 200
11 mg/kg, and blank control groups for male and female rats, respectively. Experimental rats were
12 treated with **17** through oral administration every other day for 14 days. Additionally, the body
13 weight as well as food intake were recorded. The rats were sacrificed and dissected at the end of
14 the experiment and the adrenal gland, brain, heart, kidney, liver, thymus, ovary (female), uterus
15 with cervix (female), testes (male), epididymis (male), and spleen (male) were extracted. The
16 blood was also collected and the samples analyzed by blood biochemistry assay. The blood
17 samples were centrifuged at 5000 rpm for 20 min, and the supernatant was subjected to blood
18 biochemistry experiments. Typical functional indicators were investigated, including urea, CRE
19 (creatinine), AST (aspartate aminotransferase), ALT (alanine aminotransferase), A/G (albumin/
20 globulin), GLO (globulin), ALB (albumin) and TP (total protein).
21
22
23
24
25
26
27
28
29
30
31
32
33
34
35

36 *AMES assay.* The test strains used in the mutagenicity test were *Salmonella typhimurium* strains
37 (TA98 and TA100). The test was performed in the presence or absence of the S9 metabolic
38 activation system using a six-well culture plate, with a solvent control group (DMSO) and a
39 positive control group; each treatment group had two replicates. Compound **17** was set at five
40 concentrations, ranging from 62.5 to 1000.0 µg/well. The plate was incubated at 37 °C for 48-50
41 hours and the bacterial toxicity of the test compound in each well then detected. The number of
42 mutant colonies in each well was also counted. In this test, DMSO was used to dissolve the test
43 compound **17**. In the non-S9 group (-S9), 2-nitropyrene and sodium azide were used as positive
44
45
46
47
48
49
50
51
52
53
54
55
56
57
58
59
60

controls for TA98 and TA100, respectively. In the S9 group (+ S9), 2-aminopyrene was used as TA98 and TA100 positive controls.

ASSOCIATED CONTENT

Supporting Information. The Supporting Information is available free of charge on the ACS Publication website at DOI:10.1021/acs.jmedchem.xxxxxxx.

Docked poses of **17** into PHD2 catalytic site, Cytotoxicity of **17** toward typical cells, Docking validation and overlay analysis, OPD-based inhibitory activity toward PHDs for **17**, Inhibition against typical KDMs, hERG inhibitory activity of **17**, AMES results for **17**, Spectra (NMR and HRMS) of intermediates and target compounds, HPLC assessment of purity for target compounds (PDF)

Molecular formula strings (CSV)

AUTHOR INFORMATION

Corresponding Authors

*(Q. You) Phone & Fax: +86-25-83271351. E-mail: youqd@163.com

(X. Zhang) Phone: +86-13913007140. E-mail: zxj@cpu.edu.cn

ORCID

Qidong You: 0000-0002-8587-0122

Xiaojin Zhang: 0000-0002-1898-3071

Notes

The authors declare no competing financial interest.

Author Contributions

¹ These authors contributed equally.

Notes

The authors declare no competing financial interest.

ACKNOWLEDGMENT

This work was supported by grants from the National Natural Science Foundation of China (Grant 81973173), Jiangsu Province Funds for Excellent Young Scientists (Grant BK20170088), the Open Project of State Key Laboratory of Natural Medicines (Grant SKLNMZZCX201803), the National Major Science and Technology Project of China (Grant 2017ZX09302003), and the Six Talent Peaks Project (Grant YY-023) and 333 Project of Jiangsu Province.

ABBREVIATIONS

ADME, absorption, distribution, metabolism, and excretion; CYP450, cytochrome p450; CKD, chronic kidney disease; EPO, erythropoietin; FP, fluorescence polarization; HIF, hypoxia-inducible factor; Hb, hemoglobin; HRE, hypoxia responsive element; MTT, 3-(4,5-dimethylthiazol-2-yl)-2,5-diphenyltetrazolium bromide; NMPA, National Medical Products Administration; OPD, O-Phenylenediamine; PHD, Prolyl hydroxylase; PD, pharmacodynamic; PK, pharmacokinetic; pVHL, von Hippel–Lindau; RBCs, red blood cells; 2-OG, 2-oxoglutarate.

REFERENCES

(1) Sankaran, V. G.; Weiss, M. J. Anemia: progress in molecular mechanisms and therapies. *Nat. Med.* **2015**, *21*, 221–230.

1
2
3 (2) Cornes, P.; Coiffier, B.; Zambrowski, J. J. Erythropoietic therapy for the treatment of anemia
4 in patients with cancer: a valuable clinical and economic option. *Curr. Med. Res. Opin.* **2007**, *23*,
5 357–368.
6
7

8
9 (3) Stohlawetz, P. J.; Dzirlo, L.; Hergovich, N.; Lackner, E.; Mensik, C.; Eichler, H. G.; Kabrna,
10 E.; Geissler, K.; Jilma, B. Effects of erythropoietin on platelet reactivity and thrombopoiesis in
11 humans. *Blood* **2000**, *95*, 2983–2989.
12
13

14
15 (4) Yeh, T. L.; Leissing, T. M.; Abboud, M. I.; Thinnes, C. C.; Atasoylu, O.; Holt-Martyn, J. P.;
16 Zhang, D.; Tumber, A.; Lippl, K.; Lohans, C. T.; Leung, I. K. H.; Morcrette, H.; Clifton, I. J.;
17 Claridge, T. D. W.; Kawamura, A.; Flashman, E.; Lu, X.; Ratcliffe, P. J.; Chowdhury, R.; Pugh,
18 C. W.; Schofield, C. J. Molecular and cellular mechanisms of HIF prolyl hydroxylase inhibitors in
19 clinical trials. *Chem. Sci.* **2017**, *8*, 7651–7668.
20
21
22

23
24 (5) Joharapurkar, A. A.; Pandya, V. B.; Patel, V. J.; Desai, R. C.; Jain, M. R. Prolyl hydroxylase
25 inhibitors: a breakthrough in the therapy of anemia associated with chronic diseases. *J. Med. Chem.*
26 **2018**, *61*, 6964–6982;
27
28

29
30 (6) Bruick, R. K.; McKnight, S. L. A conserved family of prolyl-4-hydroxylases that modify HIF.
31 *Science* **2001**, *294*, 1337–1340.
32
33

34
35 (7) Rabinowitz, M. H. Inhibition of hypoxia-inducible factor prolyl hydroxylase domain oxygen
36 sensors: tricking the body into mounting orchestrated survival and repair responses. *J. Med. Chem.*
37 **2013**, *56*, 9369–9402.
38
39

40
41 (8) Hon, W. C.; Wilson, M. I.; Harlos, K.; Claridge, T. D.; Schofield, C. J.; Pugh, C. W.; Maxwell,
42 P. H.; Ratcliffe, P. J.; Stuart, D. I.; Jones, E. Y. Structural basis for the recognition of
43 hydroxyproline in HIF-1 alpha by pVHL. *Nature* **2002**, *417*, 975–978.
44
45

46
47 (9) Berra, E.; Benizri, E.; Ginouves, A.; Volmat, V.; Roux, D.; Pouyssegur, J. HIF prolyl-
48 hydroxylase 2 is the key oxygen sensor setting low steady-state levels of HIF-1alpha in normoxia.
49 *The EMBO J.* **2003**, *22*, 4082–4090.
50
51

52
53 (10) Li, Z.; You, Q.; Zhang, X. Small-molecule modulators of the hypoxia-inducible factor
54 pathway: development and therapeutic applications. *J. Med. Chem.* **2019**, *62*, 5725–5749.
55
56
57

1
2
3 (11) Wu, Y.; Wang, N.; Lei, Y.; Hu, T.; You, Q.; Zhang, X. Small molecular inhibitors of HIF-
4 PHD2: a valid strategy to renal anemia treatment in clinical therapy. *Med. Chem. Comm.* **2016**, *7*,
5 1259–1452.
6
7

8
9 (12) Chen, N.; Hao, C.; Peng, X.; Lin, H.; Yin, A.; Hao, L.; Tao, Y.; Liang, X.; Liu, Z.; Xing, C.;
10 Chen, J.; Luo, L.; Zuo, L.; Liao, Y.; Liu, B. C.; Leong, R.; Wang, C.; Liu, C.; Neff, T.; Szczech,
11 L.; Yu, K. P. Roxadustat for anemia in patients with kidney disease not receiving dialysis. *N. Engl.*
12 *J. Med.* **2019**, *381*, 1001–1010.
13
14

15
16 (13) Dhillon, S. Roxadustat: first global approval. *Drugs* **2019**, *79*, 563–572.
17
18

19 (14) Chen, N.; Hao, C.; Liu, B. C.; Lin, H.; Wang, C.; Xing, C.; Liang, X.; Jiang, G.; Liu, Z.; Li,
20 X.; Zuo, L.; Luo, L.; Wang, J.; Zhao, M. H.; Liu, Z.; Cai, G. Y.; Hao, L.; Leong, R.; Wang, C.;
21 Liu, C.; Neff, T.; Szczech, L.; Yu, K. P. Roxadustat treatment for anemia in patients undergoing
22 long-term dialysis. *N. Engl. J. Med.* **2019**, *381*, 1011–1022.
23
24

25
26 (15) Web Sites: [https://ir.akebia.com/news-releases/news-release-details/akebia-therapeutics-
27 announces-approval-vadadustat-japan](https://ir.akebia.com/news-releases/news-release-details/akebia-therapeutics-announces-approval-vadadustat-japan) (accessed June 03, 2020).
28
29

30
31 (16) Web Sites: [https://www.gsk.com/en-gb/media/press-releases/gsk-submits-first-regulatory-
32 application-for-daprodustat-in-japan-for-patients-with-renal-anaemia-due-to-chronic-kidney-
33 disease](https://www.gsk.com/en-gb/media/press-releases/gsk-submits-first-regulatory-application-for-daprodustat-in-japan-for-patients-with-renal-anaemia-due-to-chronic-kidney-disease) (accessed June 03, 2020).
34
35

36
37 (17) McDonough, M. A.; Li, V.; Flashman, E.; Chowdhury, R.; Mohr, C.; Lienard, B. M.; Zondlo,
38 J.; Oldham, N. J.; Clifton, I. J.; Lewis, J.; McNeill, L. A.; Kurzeja, R. J.; Hewitson, K. S.; Yang,
39 E.; Jordan, S.; Syed, R. S.; Schofield, C. J. Cellular oxygen sensing: Crystal structure of hypoxia-
40 inducible factor prolyl hydroxylase (PHD2). *Proc. Natl. Acad. Sci. U. S. A.* **2006**, *103*, 9814–9819.
41
42

43
44 (18) Rosen, M. D.; Venkatesan, H.; Peltier, H. M.; Bembenek, S. D.; Kanelakis, K. C.; Zhao, L.
45 X.; Leonard, B. E.; Hocutt, F. M.; Wu, X.; Palomino, H. L.; Brondstetter, T. I.; Haugh, P. V.;
46 Cagnon, L.; Yan, W.; Liotta, L. A.; Young, A.; Mirzadegan, T.; Shankley, N. P.; Barrett, T. D.;
47 Rabinowitz, M. H. Benzimidazole-2-pyrazole HIF prolyl 4-hydroxylase inhibitors as oral
48 erythropoietin secretagogues. *ACS Med. Chem. Lett.* **2010**, *1*, 526–529.
49
50
51
52
53
54
55
56
57
58
59
60

1
2
3 (19) Chowdhury, R.; Candela-Lena, J. I.; Chan, M. C.; Greenald, D. J.; Yeoh, K. K.; Tian, Y. M.;
4 McDonough, M. A.; Tumber, A.; Rose, N. R.; Conejo-Garcia, A.; Demetriades, M.; Mathavan, S.;
5 Kawamura, A.; Lee, M. K.; van Eeden, F.; Pugh, C. W.; Ratcliffe, P. J.; Schofield, C. J. Selective
6 small molecule probes for the hypoxia inducible factor (HIF) prolyl hydroxylases. *ACS Chem. Biol.*
7 **2013**, *8*, 1488–1496.
8
9

10
11
12 (20) Warshakoon, N. C.; Wu, S.; Boyer, A.; Kawamoto, R.; Sheville, J.; Renock, S.; Xu, K.;
13 Pokross, M.; Evdokimov, A. G.; Walter, R.; Mekel, M. A novel series of imidazo[1,2-a]pyridine
14 derivatives as HIF-1alpha prolyl hydroxylase inhibitors. *Bioorg. Med. Chem. Lett.* **2006**, *16*,
15 5598–5601.
16
17
18

19
20 (21) Frohn, M.; Viswanadhan, V.; Pickrell, A. J.; Golden, J. E.; Muller, K. M.; Burli, R. W.;
21 Biddlecome, G.; Yoder, S. C.; Rogers, N.; Dao, J. H.; Hungate, R.; Allen, J. R. Structure-guided
22 design of substituted aza-benzimidazoles as potent hypoxia inducible factor-1alpha prolyl
23 hydroxylase-2 inhibitors. *Bioorg. Med. Chem. Lett.* **2008**, *18*, 5023–5026.
24
25
26

27
28 (22) Warshakoon, N. C.; Wu, S.; Boyer, A.; Kawamoto, R.; Sheville, J.; Bhatt, R. T.; Renock, S.;
29 Xu, K.; Pokross, M.; Zhou, S.; Walter, R.; Mekel, M.; Evdokimov, A. G.; East, S. Design and
30 synthesis of substituted pyridine derivatives as HIF-1alpha prolyl hydroxylase inhibitors. *Bioorg.*
31 *Med. Chem. Lett.* **2006**, *16*, 5616–5620.
32
33
34

35
36 (23) Warshakoon, N. C.; Wu, S.; Boyer, A.; Kawamoto, R.; Renock, S.; Xu, K.; Pokross, M.;
37 Evdokimov, A. G.; Zhou, S.; Winter, C.; Walter, R.; Mekel, M. Design and synthesis of a series
38 of novel pyrazolopyridines as HIF-1alpha prolyl hydroxylase inhibitors. *Bioorg. Med. Chem. Lett.*
39 **2006**, *16*, 5687–5690.
40
41
42

43 (24) Tegley, C. M.; Viswanadhan, V. N.; Biswas, K.; Frohn, M. J.; Peterkin, T. A.; Chang, C.;
44 Burli, R. W.; Dao, J. H.; Veith, H.; Rogers, N.; Yoder, S. C.; Biddlecome, G.; Tagari, P.; Allen, J.
45 R.; Hungate, R. W. Discovery of novel hydroxy-thiazoles as HIF-alpha prolyl hydroxylase
46 inhibitors: SAR, synthesis, and modeling evaluation. *Bioorg. Med. Chem. Lett.* **2008**, *18*,
47 3925–3928.
48
49
50
51
52
53
54
55
56
57
58
59
60

1
2
3 (25) Debenham, J. S.; Madsen-Duggan, C.; Clements, M. J.; Walsh, T. F.; Kuethe, J. T.; Reibarkh,
4 M.; Salowe, S. P.; Sonatore, L. M.; Hajdu, R.; Milligan, J. A.; Visco, D. M.; Zhou, D.; Lingham,
5 R. B.; Stickens, D.; DeMartino, J. A.; Tong, X.; Wolff, M.; Pang, J.; Miller, R. R.; Sherer, E. C.;
6 Hale, J. J. Discovery of N-[Bis(4-methoxyphenyl)methyl]-4-hydroxy-2-(pyridazin-3-
7 yl)pyrimidine-5-carboxamide (MK-8617), an orally active pan-inhibitor of hypoxia-inducible
8 factor prolyl hydroxylase 1-3 (HIF PHD1-3) for the treatment of anemia. *J. Med. Chem.* **2016**, *59*,
9 11039–11049.

10
11
12 (26) Vachal, P.; Miao, S.; Pierce, J. M.; Guiadeen, D.; Colandrea, V. J.; Wyvratt, M. J.; Salowe,
13 S. P.; Sonatore, L. M.; Milligan, J. A.; Hajdu, R.; Gollapudi, A.; Keohane, C. A.; Lingham, R. B.;
14 Mandala, S. M.; DeMartino, J. A.; Tong, X.; Wolff, M.; Steinhuebel, D.; Kieczkowski, G. R.;
15 Fleitz, F. J.; Chapman, K.; Athanasopoulos, J.; Adam, G.; Akyuz, C. D.; Jena, D. K.; Lusen, J. W.;
16 Meng, J.; Stein, B. D.; Xia, L.; Sherer, E. C.; Hale, J. J. 1,3,8-Triazaspiro[4.5]decane-2,4-diones
17 as efficacious pan-inhibitors of hypoxia-inducible factor prolyl hydroxylase 1–3 (HIF PHD1–3)
18 for the treatment of anemia *J. Med. Chem.* **2012**, *55*, 2945–2959.

19
20 (27) Deng, G.; Zhao, B.; Ma, Y.; Xu, Q.; Wang, H.; Yang, L.; Zhang, Q.; Guo, T. B.; Zhang, W.;
21 Jiao, Y.; Cai, X.; Zhang, J.; Liu, H.; Guan, X.; Lu, H.; Xiang, J.; Elliott, J. D.; Lin, X.; Ren, F.
22 Novel complex crystal structure of prolyl hydroxylase domain-containing protein 2 (PHD2): 2,8-
23 Diazaspiro[4.5]decan-1-ones as potent, orally bioavailable PHD2 inhibitors. *Bioorg. Med. Chem.*
24 **2013**, *21*, 6349–6358.

25
26 (28) Lei, Y.; Hu, T.; Wu, X.; Wu, Y.; Bao, Q.; Zhang, L.; Xia, H.; Sun, H.; You, Q.; Zhang, X.
27 Affinity-based fluorescence polarization assay for high-throughput screening of prolyl
28 hydroxylase 2 inhibitors. *ACS Med. Chem. Lett.* **2015**, *6*, 1236–1240.

29
30 (29) Lei, Y.; Hu, T.; Hu, M.; Yang, L.; Wu, Y.; Xiang, H.; Zhang, L.; Shen, L.; You, Q.; Zhang,
31 X. An improved and scalable synthesis of N-(5-(4-cyanophenyl)-3-hydroxypicolinoyl)glycine, a
32 promising PHD2 inhibitor for the treatment of anemia. *Tetrahedron Lett.* **2015**, *56*, 5017–5019.

33
34 (30) McNeill, L. A.; Bethge, L.; Hewitson, K. S.; Schofield, C. J. A fluorescence-based assay for
35 2-oxoglutarate-dependent oxygenases. *Anal. Biochem.* **2005**, *336*, 125–131.

1
2
3 (31) Polonchuk, L. Toward a new gold standard for early safety: automated temperature-controlled
4 hERG test on the patchliner. *Frontiers Pharmacol.* **2012**, *3*, 1–7.

5
6
7 (32) Gao, S.; Zhou, J.; Zhao, Y.; Toselli, P.; Li, W. Hypoxia-response element (HRE)-directed
8 transcriptional regulation of the rat lysyl oxidase gene in response to cobalt and cadmium. *Toxicol.*
9 *Sci.* **2013**, *132*, 379–389.

10
11
12 (33) Chang, K. H.; Stevenson, M. M. Comparison of murine Epo ELISA and Epo bioassays in
13 detecting serum Epo levels during anemia associated with malaria infection. *J. Immunol. Methods*
14 **2002**, *262*, 129–136.

15
16
17 (34) Wu, Y.; Jiang, Z.; Li, Z.; Gu, J.; You, Q.; Zhang, X. Click chemistry-based discovery of (3-
18 Hydroxy-5-(1H-1,2,3-triazol-4-yl) picolinoyl) glycines as orally active hypoxia-inducing factor
19 prolyl hydroxylase inhibitors with favorable safety profiles for the treatment of anemia. *J. Med.*
20 *Chem.* **2018**, *61*, 5332–5349.

21
22
23 (35) Jain, M. R.; Joharapurkar, A. A.; Pandya, V.; Patel, V.; Joshi, J.; Kshirsagar, S.; Patel, K.;
24 Patel, P. R.; Desai, R. C. Pharmacological characterization of ZYAN1, a novel prolyl hydroxylase
25 inhibitor for the treatment of anemia. *Drug Res.* **2016**, *66*, 107–112.

26
27
28 (36) Li, Y.; Yue, H.; Yang, S.; Yuan, D.; Li, L.; Zhao, J.; Zhao, L. Splenomegaly induced by
29 anemia impairs T cell movement in the spleen partially via EPO. *Mol. Immunol.* **2019**, *112*,
30 399–405.

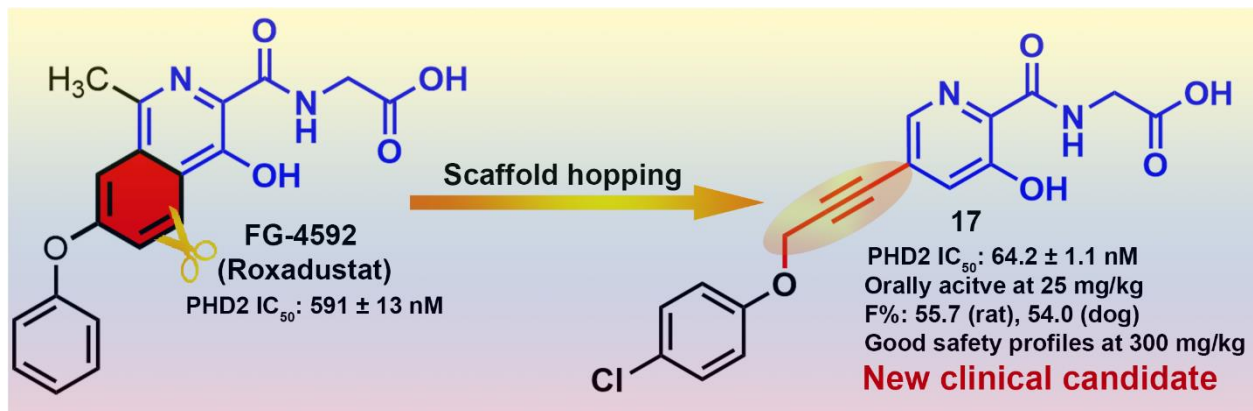


Table of Contents graphic